Systems & Control Letters 167 (2022) 105325

Contents lists available at ScienceDirect

Systems & Control Letters

journal homepage: www.elsevier.com/locate/sysconle

Trajectory tracking for nonlinear systems using extended quadratic port-Hamiltonian models without input and state coordinate transformations

N.H. Hoang [a,b,*], T.S. Nguyen [c], T.K.P. Le [d], T.T.H. Phan [e], M.A. Hussain [c], D. Dochain [f]

[a] Institute of Research and Development, Duy Tan University, Da Nang, 550000, Vietnam
[b] Faculty of Electrical-Electronic Engineering, Duy Tan University, Da Nang, 550000, Vietnam
[c] Faculty of Engineering, University Malaya, 50603 Kuala Lumpur, Malaysia
[d] University of Technology, Vietnam National University, Ho Chi Minh City, Vietnam
[e] Hanoi Pedagogical University 2, Vinh Phuc, Vietnam
[f] ICTEAM, UCLouvain, 4-6 avenue G. Lemaître, B-1348 Louvain-la-Neuve, Belgium

ARTICLE INFO

Article history:
Received 24 March 2021
Received in revised form 14 April 2022
Accepted 6 July 2022
Available online 25 July 2022

Keywords:
Quadratic port-Hamiltonian systems
Tracking control
Proportional–Integral control
Nonlinear systems

ABSTRACT

In this note, an enhanced trajectory tracking (or equivalently, tracking-error) approach is developed for the control of nonlinear systems whenever the stage of feedback passivation design prior to synthesizing state feedback controllers is impossible. To achieve this purpose while using the original state vector to retain its interpretation, it is possible without the use of input and state coordinate transformations to combine the system dynamics with the so-called extended quadratic port-Hamiltonian (PH) models (including possibly the quadratic pseudo PH models) which are then divided into non-relaxing and relaxing ones for further study on control benefits. Interestingly, both cases are associated to a unifying quadratic Hamiltonian storage function similar to that of electrical, mechanical, or electromechanical systems with a specific insight. Sufficient conditions for the global asymptotic or exponential convergence of the system trajectory to the reference one are shown. In addition, a Proportional–Integral action can be added to the tracking control for improving the closed-loop performance and robustness. The proposed approach is illustrated via two case studies, including the non-minimum phase Van de Vusse reaction system and the 3-DOF SCARA robot.

1. Introduction

Many industrial applications occur in the domains — electrical, mechanical and biochemical, etc. belonging to lumped parameter systems (i.e. with one independent variable, time, described by a set of ordinary differential equations) [1]. In some instances, the dynamics of such systems may exhibit the abnormal behaviors (such as the input/output multiplicity or limit-cycle oscillations and chaos, etc.) which are mainly caused by the highly nonlinear characteristics of multi-physics domain, irreversible thermal effects or hysteresis behavior of materials [2]. As a consequence, these behaviors give rise to strong sensitivity *w.r.t.* internal and/or external factors (such as noise/disturbance or parameter uncertainty, etc.), i.e. the sources of generating internal instabilities and therefore restrict the systems themselves to reach their desirable performance if they are operated without control [3]. Hence, during the last few decades, numerous control strategies have been proposed to tackle this theoretically difficult but interesting challenge. It is the case, for instance, for model predictive control [4], extremum-seeking control [5] and passivity-based control (PBC) [6] together with energy/power-shaping [7,8] or physics-based control approaches (e.g. [9,10] to cite a few, and references therein). Nevertheless, one of the important issues is the applicability of developed control methods for a wide range of nonlinear systems, in particular for non-minimum phase systems [11]. This is due to the fact that the non-minimum phase system has unstable zero dynamics and its stabilization cannot be achieved by using the well-known conventional approaches such as input–output linearization because asymptotic stability of these zero dynamics is a necessary condition for nominal closed-loop stability [12]. Unlike the results reported in [13,14] for which the minimum phase behavior and the output relative degree one of the given system are *a priori* required, the passivity-based control approach developed in [15,16] have considered the transversality condition instead so that feedback

* Corresponding author at: Institute of Research and Development, Duy Tan University, Da Nang, 550000, Vietnam.
E-mail addresses: hoangngocha2@duytan.edu.vn, ngocha.h@gmail.com (N.H. Hoang), KVA180023@siswa.um.edu.my (T.S. Nguyen), phungle@hcmut.edu.vn (T.K.P. Le), phanthithanhhong@hpu2.edu.vn (T.T.H. Phan), mohd_azlan@um.edu.my (M.A. Hussain), denis.dochain@uclouvain.be (D. Dochain).

https://doi.org/10.1016/j.sysconle.2022.105325
0167-6911/

passivation design is workable using an appropriate input coordinate transformation before a feedback controller is synthesized. Concretely, the feedback passivation design is first implemented in order to express the system dynamics in a structured form, called port-Hamiltonian (PH) representation, prior to developing passivity-based controllers via predefined reference dynamics. As a particular part of the reference trajectory is assigned to be a desired constant equilibrium value, this approach can be considered as a simplified version of the tracking-error-based control (TEBC) approach with generalized canonical transformations [17], whereby all the reference trajectory is time-variant. In this context, how to (i) lift restrictions on the minimum phase behavior and/or the systems fulfilling the transversality condition to be SISO and (ii) extend the TEBC approach without using input and state coordinate transformations for the stabilization of non-minimum phase nonlinear MIMO systems is a key challenge in the control research field, and it is the primary objective of this work.

Note that PH representation has been first considered for mechanical and electrical systems such as mass–spring–damper systems and series/parallel *RLC* circuits, etc. (see e.g. [18,19]). For those systems, the PH formulations are explicitly associated with a unified quadratic Hamiltonian potential[1]

$$\mathcal{H}(\boldsymbol{x}) \triangleq \frac{1}{2}\boldsymbol{x}^{\top} R_{di}\boldsymbol{x}, \tag{1}$$

where $\boldsymbol{x}$ and $\top$ are the system state vector and matrix transpose, respectively, and $R_{di} = R_{di}^{\top} > 0$. Hence the adaptation of the unified potential (1) to the port-based modeling of chemical processes[2] is the secondary objective of this work.

In this work, an unstable non-minimum phase nonlinear chemical system known as Van de Vusse reaction system (see also [25–27]) is used together with a mechanical system to illustrate the developments. It is important to note that the heat effects in such systems have to be considered properly in the treatment because the temperature is one of the major concerns of the thermal–material coupling, thereby describing the interaction of rate processes (reaction kinetics, heat transfer) and leading to non-minimum phase behavior. From a modeling perspective, the inclusion of the temperature may change the PH representation of the system from one non-relaxing form to another. The contributions of this paper are twofold:

- A class of extended quadratic PH systems (including the quadratic pseudo PH systems) is introduced. Under certain conditions, the original dynamics can be formatted into this class, and associated to a unified quadratic potential (1) without input and state coordinate transformations as in [28,29].
- A standard and flexible framework of the enhanced TEBC approach for the stabilization of the extended quadratic PH systems is developed based on the error-state dynamics preserving the port-Hamiltonian structure. It is shown that the global asymptotic or exponential stability of the TEBC can be achieved depending on the relaxing or non-relaxing nature of the considered quadratic PH system. On the other hand, for nonlinear systems with equilibrium and over a wide range of applications, different functions of time with either time-finite or exponential/asymptotic stability are proposed for reference states to be tracked. Also, an addition of the Proportional–Integral action to the error-state system is proposed not only to preserve the PH structure but also to improve the control performance and robustness. These extensions, therefore, complete the results developed in previous work [30,31].

It should be pointed out that the enhanced trajectory tracking control framework developed in this paper is different compared to others available in the literature [17,32]. Three of the key differences are summarized as follows, (i) under a so-called separability condition there is no need to determine a time/state-dependent transformation by solving a set of partial differential equations (PDEs)[3] in order to transform the error dynamics into a PH representation [17,33,34], (ii) no additional restrictions (such as closed-loop interconnection and damping matrices to be constant) are imposed on the closed-loop system while the desired trajectory is fixed or predefined [32] and (iii) the quadratic Hamiltonian may also have a clear physical meaning as extended to chemical reaction systems.

This paper is organized as follows. Section 2 briefly introduces a large class of the so-called extended PH models of affine nonlinear systems. An enhanced TEBC approach is then developed for the class of systems considered. The illustrations including numerical simulations for the tracking control design of the Van de Vusse reaction system and the 3-DOF SCARA robot are given in Section 3 to illustrate the results. It is interesting to note that while the reaction system will be stabilized at an optimal equilibrium point, the dynamics of the robot will track a desired oscillatory reference trajectory.

2. The control design of extended PH systems

Throughout this paper, we consider nonlinear dynamical systems that are affine in the control input u and whose dynamics are given by the following set of ordinary differential equations (ODEs) [6,11,12]:

$$\dot{\boldsymbol{x}} = f(\boldsymbol{x}) + g(\boldsymbol{x})\, u, \quad \boldsymbol{x}(t=0) = \boldsymbol{x}^0 \tag{2}$$

where $\boldsymbol{x} = \boldsymbol{x}(t)$ is the state vector contained in the operating region $\mathbb{D} \subseteq \mathbb{R}^n$, $f(\boldsymbol{x}) \in \mathbb{R}^n$ expresses the vector-valued smooth nonlinear function *w.r.t.* $\boldsymbol{x}$. The full rank input-state matrix and the control input are represented by $g(\boldsymbol{x}) \in \mathbb{R}^{n\times m}$ and $u \in \mathbb{R}^m$, $m \leq n$, respectively.

2.1. About extended port-Hamiltonian (PH) systems

An extension of port-based network modeling of physical systems[4] allows to re-express $f(\boldsymbol{x})$ in (2) as a decomposition of the product of some structurally extended matrices and the gradient of certain extended potential function *w.r.t.* $\boldsymbol{x}$, i.e. the co-state variables

$$f(\boldsymbol{x}) \triangleq [J(\boldsymbol{x}) - R(\boldsymbol{x})]\, \frac{\partial \mathcal{H}(\boldsymbol{x})}{\partial \boldsymbol{x}} \tag{3}$$

where $J(\boldsymbol{x})$ and $R(\boldsymbol{x})$ are called the $n\times n$ skew-symmetric extended interconnection matrix (i.e. $J(\boldsymbol{x}) = -J(\boldsymbol{x})^{\top}$) and the $n \times n$ symmetric extended damping matrix (i.e. $R(\boldsymbol{x}) = R(\boldsymbol{x})^{\top}$), respectively, while $\mathcal{H} : \mathbb{D} \longrightarrow \mathbb{R}$ presents the extended Hamiltonian storage function (possibly related to the total energy of the system). From

[1] The Hamiltonian storage function (1) is equal to the total energy of the system (i.e. it characterizes the amount of the elastic potential energy of the spring and the kinetic energy of the body or the energies stored in capacitor and inductor in case of a mass–spring–damper system or series *RLC* circuit, respectively). We refer the reader to Batlle [20] for a similar description of coupled electro-magneto-mechanical systems (for example, a magnetic levitation system). In general, the PH representation with (1) belongs to the so-called quadratic PH system [21,22].

[2] Consequently, it also has a clear physical meaning because of its link with the inventory-based storage function of chemical processes [23,24].

[3] This challenging task is time consuming and not easy to carry out.

[4] See, e.g. [18] for conservative mechanical systems governed by the Euler–Lagrange equations of motion with independent storage elements.

a mathematical point of view, (3) can generally be considered as the separability condition[5] and extensively used in particular in [38] for lumped parameter process systems.

In addition to (3), the dynamics (2) is then completed with the output defined by $y \triangleq g(\boldsymbol{x})^\top \frac{\partial \mathcal{H}(\boldsymbol{x})}{\partial \boldsymbol{x}} \in \mathbb{R}^m$ so that the resulting representation

$$\begin{cases} \dot{\boldsymbol{x}} = [J(\boldsymbol{x}) - R(\boldsymbol{x})] \frac{\partial \mathcal{H}(\boldsymbol{x})}{\partial \boldsymbol{x}} + g(\boldsymbol{x})\boldsymbol{u} \\ y = g(\boldsymbol{x})^\top \frac{\partial \mathcal{H}(\boldsymbol{x})}{\partial \boldsymbol{x}} \end{cases} \tag{4}$$

verifies the following equality:

$$\frac{d\mathcal{H}(\boldsymbol{x})}{dt} = -\left[\frac{\partial \mathcal{H}(\boldsymbol{x})}{\partial \boldsymbol{x}}\right]^\top R(\boldsymbol{x}) \frac{\partial \mathcal{H}(\boldsymbol{x})}{\partial \boldsymbol{x}} + u^\top y \tag{5}$$

This work focuses on a large class of the extended PH models (including also the so-called pseudo PH models) that is defined on the basis of the positive semi-definiteness property of the damping structure matrix $R(\boldsymbol{x})$. This concept is summarized in Definition 1.

Definition 1. The structured form (4) belongs to the class of extended PH models (EPH models, denoted by $\mathcal{H}_e$) if it satisfies one of the following two constraints:

(i) The matrix $R(\boldsymbol{x})$ is positive semi-definite, i.e.:

$$\forall \boldsymbol{v} \in \mathbb{R}^n,\ \boldsymbol{v} \neq 0,\ \ \boldsymbol{v}^\top R(\boldsymbol{x}) \boldsymbol{v} \ \geq \ 0 \tag{6}$$

(ii) Or $R(\boldsymbol{x})$ is negative semi-definite or indefinite (i.e. neither positive nor negative semi-definite).

The structure (4) fulfilling (i) is a standard PH representation [19] and considered here as a non-relaxed EPH model. Otherwise, (4) with (ii) is a pseudo PH representation and considered here as a relaxed EPH model [39]. It is worth noting that the class of EPH models considered here is particular but large because it encompasses both the non-relaxed (i.e. standard) and relaxed (i.e. pseudo) PH models, thereby allowing the development of a flexible TEBC approach with specific control benefits. We shall not elaborate any further on the existence of the EPH models here and for a system-theoretic treatment, we refer the reader to e.g. [18] (see also [40] for an extensive exposition and a large number of references).

Let $\mathcal{H}_{e,nr}$ and $\mathcal{H}_{e,r}$ be the (disjoint) subclasses of $\mathcal{H}_e$ which encompass the non-relaxed and relaxed EPH models, respectively. For all models belonging to either $\mathcal{H}_{e,nr}$ or $\mathcal{H}_{e,r}$, and for the sake of brevity, the argument $\frac{\partial \mathcal{H}(\boldsymbol{x})}{\partial \boldsymbol{x}}$ (if any) has been omitted from R (and J) since there is no doubt as to what the non-relaxed/relaxed EPH model is and $\frac{\partial \mathcal{H}(\boldsymbol{x})}{\partial \boldsymbol{x}}$ is a vector-valued function *w.r.t.* $\boldsymbol{x}$ explicitly.

We make the following assumption regarding systems with equilibrium.

Assumption 1 (*Feasibility Condition for Systems with Equilibrium*)**.** Given $u_\star \in \mathbb{R}^m$, the set $\mathcal{E}_\star$ defined by $\mathcal{E}_\star = \left\{ \boldsymbol{x}_\star \middle| [J(\boldsymbol{x}_\star) - R(\boldsymbol{x}_\star)] \frac{\partial \mathcal{H}(\boldsymbol{x}_\star)}{\partial \boldsymbol{x}} + g(\boldsymbol{x}_\star) u_\star = 0 \right\}$ exists. Also, $\boldsymbol{x}_\star \in \mathcal{E}_\star$ is said to be an equilibrium point (or the steady state value) corresponding to $u_\star$.

Assumption 1 is clearly fulfilled for nonlinear systems (such as chemical reaction systems), of which at least one equilibrium point is present when time becomes very large or goes to infinity [10,15,25,41]. This assumption is no longer valid for systems having the oscillatory behavior (i.e. the limit cycle) [42,43] or systems without equilibrium [44].

[5] Solutions for such a separability can be found using the orthogonal decomposition method [22], the dual Brayton–Moser formulation [35,36] or the Hodge decomposition technique [37]. Importantly, the orthogonal decomposition method [22] allows transforming $f(\boldsymbol{x})$ into the form (3) without solving PDEs. Note, however, that in this method the input coordinate transformation may be required.

2.2. An enhanced tracking-error-based control approach

For the sake of deriving the main results in the remaining of the paper, let $\mathcal{I}$ be the subset having m elements derived from the set $\mathbb{N}$ of ordered indices, $\mathbb{N} = \{1, \ldots, n\}$. An additional assumption related to the zero-state detectability condition is considered.

Assumption 2 (*Zero-State Detectability [17]*)**.** Given some reachable desired equilibrium, say $\boldsymbol{x}_{\star r} \in \mathcal{E}_\star$. Let x_i and $x_{\star r,i}$ respectively be the ith elements of $\boldsymbol{x}$ and $\boldsymbol{x}_{\star r}$, and consider a suitable selection $\mathcal{I}$ of $\mathbb{N}$, if $x_i \to x_{\star r,i},\ i \in \mathcal{I}$ as $t \to +\infty$ then $\lim_{t\to+\infty} x_j(t) = x_{\star r,j},\ j \in \mathcal{J} = \mathbb{N} \setminus \mathcal{I}$.

Assumption 2 may be interpreted as follows. At the steady state, there exists $\boldsymbol{x}_{\star r}$ associated with $u_{\star r}$ satisfying $F_l(\boldsymbol{x}_{\star r}, u_{\star r}) = 0$ with F_l, $l = 1, 2, \ldots, n$, being nonlinear functions derived from the state steady condition $f(\boldsymbol{x}_{\star r}) + g(\boldsymbol{x}_{\star r}) u_{\star r} = 0$. Consequently, using the implicit function theorem it may be possible to represent $x_{\star r,j} = G_j\big((\boldsymbol{x}_{\star r})_{\mathcal{I}}, u_{\star r}\big)$ with G_j being a nonlinear function of only $(\boldsymbol{x}_{\star r})_{\mathcal{I}}$[6] and $u_{\star r}$, and $x_{\star r,j},\ j \in \mathcal{J}$, are well-defined and unique. This assumption is generally satisfied in accordance with common physical knowledge. This is for instance the case for the temperature of reaction systems with the chemical kinetics governed by mass-action law [25]. In addition, its validity still holds for hydraulic systems and many others (possibly even with input or output multiplicity behavior) (see e.g. [28,38]). Hence it will pose no real restriction on the class of considered systems. From a mathematical point of view, it implies that the system can be fully controlled by acting on $x_i,\ i \in \mathcal{I}$ only. The zero-state detectability assumption can be alternatively and more generally stated that if $\big(\boldsymbol{x}(t)\big)_{\mathcal{I}} \to \big(\boldsymbol{x}_d(t)\big)_{\mathcal{I}}$ as $t \to +\infty$ then $\lim_{t\to+\infty} \big(\boldsymbol{x}(t)\big)_{\mathcal{J}} = \big(\boldsymbol{x}_d(t)\big)_{\mathcal{J}}$, where $\boldsymbol{x}_d(t)$ is some reference trajectory (for example, it reaches the desired setpoint as time goes to infinity). The following theorem presents our main result in its full generality, but in a rather conceptual and flexible form for the tracking control of the EPH model (4) of the dynamics (2) using an enhanced tracking-error-based control (TEBC) approach.

Theorem 1. *Assume that:*

(i) *The dynamics (2) possesses an EPH model described by (4) (i.e. $\in \mathcal{H}_{e,nr}$ or $\in \mathcal{H}_{e,r}$) and the Hamiltonian storage function $\mathcal{H}(\boldsymbol{x})$ is given by (1);*

(ii) *A generalized reference trajectory $\boldsymbol{x}_d$ is governed by*

$$\dot{\boldsymbol{x}}_d \triangleq \left[J(\boldsymbol{x}) - R(\boldsymbol{x})\right] \frac{\partial \mathcal{H}(\boldsymbol{x}_d)}{\partial \boldsymbol{x}_d} + R_l(\boldsymbol{x}) \frac{\partial \mathscr{H}(\boldsymbol{e}_r)}{\partial \boldsymbol{e}_r} + g(\boldsymbol{x}) u \tag{7}$$

where $\boldsymbol{e}_r \triangleq \boldsymbol{x} - \boldsymbol{x}_d$ is the error-state vector, $\mathscr{H}(\boldsymbol{e}_r) \triangleq \frac{1}{2} \boldsymbol{e}_r^\top R_{di} \boldsymbol{e}_r$, $\mathcal{H}(\boldsymbol{x}_d) = \frac{1}{2} \boldsymbol{x}_d^\top R_{di} \boldsymbol{x}_d$ and $R_l(\boldsymbol{x})$ is the generalized damping injection (i.e. $R_l(\boldsymbol{x}) = R_l(\boldsymbol{x})^\top$).

Then if $\boldsymbol{x} \in \mathcal{H}_{e,nr}$, $\boldsymbol{x}$ converges globally exponentially to $\boldsymbol{x}_d$ with a decay constant bounded by $c_d = 2\frac{\lambda}{\beta}$ where:

$$\lambda = \inf_{\boldsymbol{x} \in \mathbb{D}} \left(\mathrm{eig}\left(R_{di} R_l(\boldsymbol{x}) R_{di} \right) \right) \tag{8}$$

and

$$\beta = \sup_{\boldsymbol{x} \in \mathbb{D}} \left(eig\,(R_{di}) \right) \tag{9}$$

if the following condition is met

$$R_l(\boldsymbol{x}) > 0 \tag{10}$$

[6] The notation $(.)_{\mathcal{I}}$ stands for a subvector (or generally, a submatrix) extracted from $(.)$ by selecting elements corresponding to row i, $i \in I$.

Otherwise, when $\boldsymbol{x} \in \mathcal{H}_{e,r}$, *the global asymptotic convergence of* $\boldsymbol{x}$ *to* $\boldsymbol{x}_d$ *is guaranteed if* $R_l(\boldsymbol{x})$ *is chosen so that the following condition holds:*

$$R(\boldsymbol{x}) + R_l(\boldsymbol{x}) = \Big(R(\boldsymbol{x}) + R_l(\boldsymbol{x})\Big)^\top > 0 \tag{11}$$

For any case, assume that the selection $\mathcal{I}$ *is made available, thus guaranteeing that a submatrix* $g_s(\boldsymbol{x})$ *extracted from* $g(\boldsymbol{x})$, *i.e.* $g_s(\boldsymbol{x}) \triangleq \big(g(\boldsymbol{x})\big)_{\mathcal{I}}$, *is invertible then* $\boldsymbol{x}$ *converges globally to the desired reference* $\boldsymbol{x}_d$ *using the feedback law given by* $u = \beta(\boldsymbol{x}, \boldsymbol{x}_d)$ *with*

$$\beta(\boldsymbol{x}, \boldsymbol{x}_d) = g_s(\boldsymbol{x})^{-1}\left(\dot{\boldsymbol{x}}_d - \Big[J(\boldsymbol{x}) - R(\boldsymbol{x})\Big]\frac{\partial \mathcal{H}(\boldsymbol{x}_d)}{\partial \boldsymbol{x}_d} - R_l(\boldsymbol{x})\frac{\partial \mathscr{H}(\boldsymbol{e}_r)}{\partial \boldsymbol{e}_r}\right)_{\mathcal{I}} \tag{12}$$

where $(\boldsymbol{x}_d)_{\mathcal{I}}$ *is predefined as a function of time while* $(\boldsymbol{x}_d)_{\mathcal{J}}$ *is constructed from the following expression*

$$(\dot{\boldsymbol{x}}_d)_{\mathcal{J}} = \left(\Big[J(\boldsymbol{x}) - R(\boldsymbol{x})\Big]\frac{\partial \mathcal{H}(\boldsymbol{x}_d)}{\partial \boldsymbol{x}_d} + R_l(\boldsymbol{x})\frac{\partial \mathscr{H}(\boldsymbol{e}_r)}{\partial \boldsymbol{e}_r} + g(\boldsymbol{x})\beta(\boldsymbol{x}, \boldsymbol{x}_d)\right)_{\mathcal{J}}. \tag{13}$$

Proof. The idea of the proof is to prove that $\boldsymbol{x}_d$ converges to $\boldsymbol{x}_{\star r}$ in finite-time or when time goes to infinity, while the system trajectory $\boldsymbol{x}$ tracks $\boldsymbol{x}_d$. Indeed, it can be shown that the time derivative of $\mathscr{H}(\boldsymbol{e}_r)$ is expressed by $\dot{\mathscr{H}}(\boldsymbol{e}_r) = \left[\frac{\partial \mathscr{H}(\boldsymbol{e}_r)}{\partial \boldsymbol{e}_r}\right]^\top \dot{\boldsymbol{e}}_r$. On the other hand, the error state vector dynamics is[7]

$$\dot{\boldsymbol{e}}_r = \Big\{J(\boldsymbol{x}) - [R(\boldsymbol{x}) + R_l(\boldsymbol{x})]\Big\}\frac{\partial \mathscr{H}(\boldsymbol{e}_r)}{\partial \boldsymbol{e}_r} \tag{14}$$

where $\frac{\partial \mathcal{H}(\boldsymbol{x})}{\partial \boldsymbol{x}} - \frac{\partial \mathcal{H}(\boldsymbol{x}_d)}{\partial \boldsymbol{x}_d} = R_{di}(\boldsymbol{x} - \boldsymbol{x}_d) = R_{di}\boldsymbol{e}_r = \frac{\partial \mathscr{H}(\boldsymbol{e}_r)}{\partial \boldsymbol{e}_r}$, the first entry of (4) and Eq. (7) have been used. Consequently, one has

$$\dot{\mathscr{H}}(\boldsymbol{e}_r) = -\left[\frac{\partial \mathscr{H}(\boldsymbol{e}_r)}{\partial \boldsymbol{e}_r}\right]^\top [R(\boldsymbol{x}) + R_l(\boldsymbol{x})]\frac{\partial \mathscr{H}(\boldsymbol{e}_r)}{\partial \boldsymbol{e}_r} \tag{15}$$

First, if $\boldsymbol{x} \in \mathcal{H}_{e,nr}$, i.e. $R(\boldsymbol{x}) = R(\boldsymbol{x})^\top \geq 0$, the following (strict) inequality holds

$$\dot{\mathscr{H}}(\boldsymbol{e}_r) \leq -\left[\frac{\partial \mathscr{H}(\boldsymbol{e}_r)}{\partial \boldsymbol{e}_r}\right]^\top R_l(\boldsymbol{x})\frac{\partial \mathscr{H}(\boldsymbol{e}_r)}{\partial \boldsymbol{e}_r} < 0 \tag{16}$$

since $R_l(\boldsymbol{x}) = R_l(\boldsymbol{x})^\top > 0$. The exponential convergence property of the system trajectory $\boldsymbol{x}$ to the reference trajectory $\boldsymbol{x}_d$ is straightforward. Indeed from (16) and since $\frac{\partial \mathscr{H}(\boldsymbol{e}_r)}{\partial \boldsymbol{e}_r} = R_{di}\boldsymbol{e}_r$ one obtains $\dot{\mathscr{H}}(\boldsymbol{e}_r) \leq -\boldsymbol{e}_r{}^\top R_{di}R_l(\boldsymbol{x})R_{di}\boldsymbol{e}_r$. Hence

$$\dot{\mathscr{H}}(\boldsymbol{e}_r) \leq -\lambda \boldsymbol{e}_r{}^\top \boldsymbol{e}_r \tag{17}$$

with λ defined by (8). By $\mathscr{H}(\boldsymbol{e}_r) = \frac{1}{2}\boldsymbol{e}_r{}^\top R_{di}\boldsymbol{e}_r$, it gives $\mathscr{H}(\boldsymbol{e}_r) > 0$ and $\boldsymbol{e}_r{}^\top \boldsymbol{e}_r > \frac{2}{\beta}\mathscr{H}(\boldsymbol{e}_r)$ where β is defined in (9). Therefore (17) becomes $\dot{\mathscr{H}}(\boldsymbol{e}_r) \leq -2\frac{\lambda}{\beta}\mathscr{H}(\boldsymbol{e}_r) < 0$. Since $\dot{\mathscr{H}}(\boldsymbol{e}_r)$ is negative and (radially) bounded above by itself, it follows immediately that $\boldsymbol{e}_r \to \boldsymbol{0}$ as $t \to \infty$ with some exponential decay c_d. Alternatively, if $\boldsymbol{x} \in \mathcal{H}_{e,r}$, (15) yields $\dot{\mathscr{H}}(\boldsymbol{e}_r) < 0$ thanks to (11). The error dynamics (14) is then globally asymptotically stabilized at the origin by invoking the LaSalle's invariance principle [12] since the largest invariant set contained in $\{\boldsymbol{e} \,|\, \boldsymbol{e}^\top R_{di}\boldsymbol{e} = 0\}$ equals $\boldsymbol{0}$. On the other hand, one has from (7)

$$\big(\dot{\boldsymbol{x}}_d\big)_{\mathcal{I}} = \left(\Big[J(\boldsymbol{x}) - R(\boldsymbol{x})\Big]\frac{\partial \mathcal{H}(\boldsymbol{x}_d)}{\partial \boldsymbol{x}_d} + R_l(\boldsymbol{x})\frac{\partial \mathscr{H}(\boldsymbol{e}_r)}{\partial \boldsymbol{e}_r} + g(\boldsymbol{x})u\right)_{\mathcal{I}} \tag{18}$$

[7] Obviously, the dynamics of the error state vector $\boldsymbol{e}$ given by (14) belongs to an extended PH structure, i.e. $\boldsymbol{e}_r \in \mathcal{H}_e$. As shown, the derivation of this structural form is straightforward and the Hamiltonian is explicit without using generalized canonical transformations as compared to [17].

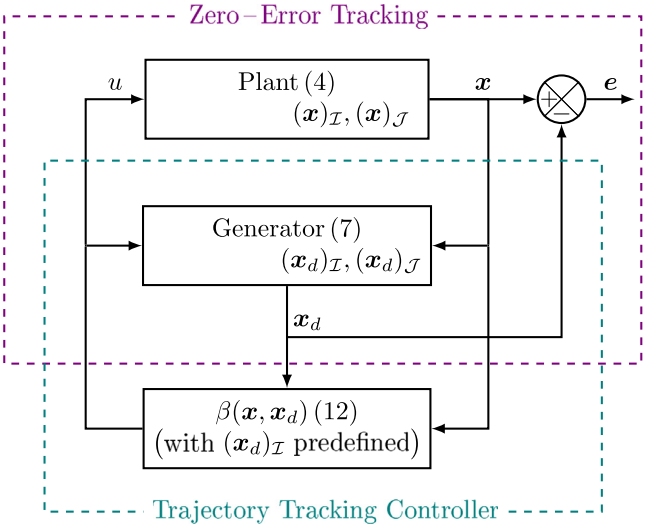

Fig. 1. Tracking control system model.

$$\big(\dot{\boldsymbol{x}}_d\big)_{\mathcal{J}} = \left(\Big[J(\boldsymbol{x}) - R(\boldsymbol{x})\Big]\frac{\partial \mathcal{H}(\boldsymbol{x}_d)}{\partial \boldsymbol{x}_d} + R_l(\boldsymbol{x})\frac{\partial \mathscr{H}(\boldsymbol{e}_r)}{\partial \boldsymbol{e}_r} + g(\boldsymbol{x})u\right)_{\mathcal{J}} \tag{19}$$

Once $(\boldsymbol{x}_d)_{\mathcal{I}}$ is predefined, using the matching Eq. (18) one obtains (12) that in turn allows the construction of $(\boldsymbol{x}_d)_{\mathcal{J}}$ via (13) prior to implementing the feedback law $\beta(\boldsymbol{x}, \boldsymbol{x}_d)$. The latter completes the proof provided that Assumption 2 holds. ■

Remark 1. At the stage of control design, one assigns $x_{d,i}(t),\ i \in \mathcal{I}$, directly as predefined functions of time (one thus has $\dot{x}_{d,i}(t),\ i \in \mathcal{I}$). For systems with the desired (constant) setpoint, one possibility is to assign $\dot{x}_{d,i}$ first, i.e.

$$\dot{x}_{d,i} = r_{d,i}(x_{d,i}, x_{\star r,i}) \text{ subject to } x_{d,i}(+\infty) = x_{\star r,i},\ i \in \mathcal{I} \tag{20}$$

with $r_{d,i}$ being a function satisfying $r_{d,i}(x_{\star r,i}, x_{\star r,i}) = 0$. Once $r_{d,i}(x_{d,i}, x_{\star r,i})$ in (20) is explicitly made, the time derivatives of $x_{d,i},\ i \in \mathcal{I}$, are determined. For the sake of illustration, $r_{d,i}(x_{d,i}, x_{\star r,i})$ can be chosen so that (20) yields

$$\dot{x}_{d,i} = -\kappa_i(x_{d,i} - x_{\star r,i})^{\gamma_i},\ i \in \mathcal{I} \tag{21}$$

with the scalars $\kappa_i > 0$ and $\gamma_i > 0$. As a result, there exists a finite-time and asymptotic convergence solution to (21) when $0 < \gamma_i < 1$, that is, $x_{d,i}(t) = x_{\star r,i} + \left(-\delta_i\kappa_i t + (x_{d,i}^0 - x_{\star r,i})^{\delta_i}\right)^{\frac{1}{\delta_i}},\ 0 \leq t \leq \tau$ or $x_{d,i}(t) = x_{\star r,i},\ t > \tau$ with $\delta_i = 1 - \gamma_i > 0$ and the finite-time constant τ given by $\tau \triangleq \frac{(x_{d,i}^0 - x_{\star r,i})^{\delta_i}}{\delta_i\kappa_i} > 0$. There is exponential convergence given by $x_{d,i}(t) = x_{\star r,i} + (x_{d,i}^0 - x_{\star r,i})\exp(-\kappa_i t),\ \forall t \geq 0$ if $\gamma_i = 1$. Otherwise, an asymptotic convergence solution is derived if $\gamma_i > 1$. Note that it is also possible to generate damped oscillations (decreasing amplitude) of the reference states $x_{d,i}(t),\ i \in \mathcal{I}$, with

$$\dot{x}_{d,i} = -\frac{c_1}{c_2}(x_{d,i} - x_{\star r,i}) - \frac{c_0}{c_2}\int_0^t \big(x_{d,i}(t') - x_{\star r,i}\big)dt' \tag{22}$$

with $c_0c_1 > 0$, $c_0c_2 > 0$ and $0 < \frac{1}{2}\frac{c_1}{c_0}\sqrt{\frac{c_0}{c_2}} < 1$.

Fig. 1 summarizes the main features of the proposed tracking control theory. As shown, this encompasses two crucial blocks, namely the Zero-Error Tracking (ZET) and Trajectory Tracking Controller (TTC) blocks. The ZET block guarantees a global convergence of the error state vector $\boldsymbol{e}$ to the zero vector as time goes to infinity, while the TTC block synthesizes a smooth (or, at

least, continuous) control law using a partially predefined, desired trajectory to achieve trajectory tracking under the assumption of zero-state detectability.

Remark 2. As the extended dynamics

$$\begin{bmatrix} \dot{\boldsymbol{e}}_r \\ \cdot \\ -\int_0^t g^\top \frac{\partial \mathscr{H}}{\partial \boldsymbol{e}_r} dt' \end{bmatrix} = \begin{bmatrix} J - \left[R + R_I + g\, K_{\mathrm{di,P}}\, g^\top\right] & g \\ -g^\top & 0 \end{bmatrix} \begin{bmatrix} \frac{\partial \mathscr{H}}{\partial \boldsymbol{e}_r} \\ -K_{\mathrm{di,I}} \int_0^t g^\top \frac{\partial \mathscr{H}}{\partial \boldsymbol{e}_r} dt' \end{bmatrix} \tag{23}$$

is stable because $W = \mathscr{H} + \left(\int_0^t g^\top \frac{\partial \mathscr{H}}{\partial \boldsymbol{e}_r} dt'\right)^\top K_{\mathrm{di,I}} \left(\int_0^t g^\top \frac{\partial \mathscr{H}}{\partial \boldsymbol{e}_r} dt'\right)$ is a strict Lyapunov function, the stabilization of $\boldsymbol{e}_r$ at the origin remains valid using a more general form of the control input, i.e.

$$u = \beta(\boldsymbol{x}, \boldsymbol{x}_d) + v \tag{24}$$

with $\beta(\boldsymbol{x}, \boldsymbol{x}_d)$ given in (12) and v being a coupled Proportional–Integral (PI) action below

$$v = -K_{\mathrm{di,P}}\, g(\boldsymbol{x})^\top \frac{\partial \mathscr{H}(\boldsymbol{e}_r)}{\partial \boldsymbol{e}_r} - K_{\mathrm{di,I}} \int_0^t g\big(\boldsymbol{x}(t')\big)^\top \frac{\partial \mathscr{H}\big(\boldsymbol{e}_r(t')\big)}{\partial \boldsymbol{e}_r} dt' \tag{25}$$

where $K_{\mathrm{di,P}}$ and $K_{\mathrm{di,I}}$ are the $m \times m$ matrices fulfilling $K_{\mathrm{di,P}} = K_{\mathrm{di,P}}^\top \geq 0$ and $K_{\mathrm{di,I}} = K_{\mathrm{di,I}}^\top \geq 0$. It should be also noted that this generalizes the integral action presented in previous work [17]. However, unlike the former, the latter directly acts on the error-state system while still preserving the pH format.

Remark 3. Despite the fact that the desired equilibrium may not be at the origin, and the input and output variables of the system take nonzero values at steady state, the enhanced TEBC approach proposed here simply relies on a straightforward derivation of the reference trajectory with suitable damping injection for the error tracking algorithm, and thereby remaining unaffected by the dissipation obstacle as compared with the previous PBC approaches (for instance, the energy-balancing PBC design fails when applied to a parallel *RLC* circuit [7,19]).

3. Case studies

3.1. Case study 1: A chemical system with equilibrium

3.1.1. The mathematical model and system analysis

We consider the Van de Vusse reaction scheme in a continuous stirred tank reactor, as described in [25–27]

$$\begin{aligned} &\underbrace{C_5H_6}_{S_1} \xrightarrow{k_1} \underbrace{C_5H_7OH}_{S_2} \xrightarrow{k_2} \underbrace{C_5H_8(OH)_2}_{S_3} \\ &2\ \underbrace{C_5H_6}_{S_1} \xrightarrow{k_3} \underbrace{C_{10}H_{12}}_{S_4} \end{aligned} \tag{26}$$

where cyclopentadiene (species S_1) and cyclopentenol (species S_2) are the reactant and main product, respectively. Species S_2 is considered as the product of interest. The two other products are cyclopentanediol (species S_3) and dicyclopentadiene (species S_4). The reactor model consists of material balances for species S_1 and S_2, and an energy balance, as described by (2) with $\boldsymbol{x} = (x_1, x_2, x_3)^\top$ [25–27],

$$f(\boldsymbol{x}) = \begin{bmatrix} -k_1 x_1 - 2k_3 x_1^2 \\ k_1 x_1 - k_2 x_2 \\ \frac{-\Delta H_1 k_1 x_1 - \Delta H_2 k_2 x_2 - 2\Delta H_3 k_3 x_1^2}{\rho C_p} \end{bmatrix}, \tag{27}$$

$$g(\boldsymbol{x}) = \begin{bmatrix} (x_{10} - x_1) & 0 \\ -x_2 & 0 \\ (x_{30} - x_3) & \frac{1}{\rho C_p} \end{bmatrix} \text{ and } u = \begin{bmatrix} u_1 \\ u_2 \end{bmatrix} \tag{28}$$

where u_1 and u_2 are the dilution rate and the heat removal rate, respectively. All process parameters, their significance and numerical values are listed in Appendix A. Note that the molar concentration of each species is always smaller than the inlet molar concentration and the absolute temperature is positive [41], the operating region of the states is thus given as $\mathbb{D} = (0 \quad x_{10})^2 \times (0 \quad +\infty)$.

Also k_1, k_2 and k_3 in (27) are the reaction kinetics and governed by the Arrhenius equation below

$$k_i(x_3) = k_{i0} \exp\left(\frac{-E_i}{R x_3}\right), \quad i = 1, 2, 3 \tag{29}$$

Assume that the reactor is initially operated corresponding to the nominal conditions $u_{\star,1} = 19.52$ (1/h) and $u_{\star,2} = -500$ (kJ/(l.h)). The equilibrium point $\boldsymbol{x}_\star$ is then calculated by $\boldsymbol{x}_\star = (1.25, 0.86, 404.7)^\top$. In this case, the zero of the transfer function of the linearized system from u_2 to x_2 is found to be $+89.11$. This indicates that the process is locally non-minimum phase around the given equilibrium. As a consequence, it prevents input–output linearization technique [12] and previous PBC approaches such as [13,14] from controlling the system because of the unstable zero dynamics of the system. In what follows, we shall show the way to apply the proposed enhanced TEBC theory as per Theorem 1 without using input and/or state coordinate transformations as compared with previous works [15–17,28].

3.1.2. The steady-state optimization problem

The following three equalities hold at the steady state:

$$\begin{cases} F_1 \triangleq x_{\star,1} - \frac{-(k_{\star,1}+u_{\star,1}) + \sqrt{(k_{\star,1}+u_{\star,1})^2 + 8k_{\star,3}x_{10}u_{\star,1}}}{4k_{\star,3}} = 0 \\ F_2 \triangleq x_{\star,2} - \frac{k_{\star,1}}{k_{\star,2}+u_{\star,1}} x_{\star,1} = 0 \\ F_3 \triangleq (\Delta H_1 k_{\star,1} + \Delta H_2 \frac{k_{\star,1}k_{\star,2}}{k_{\star,2}+u_{\star,1}}) x_{\star,1} \\ \qquad + 2\Delta H_3 k_{\star,3} x_{\star,1}^2 - \rho C_p \left(x_{30} - x_{\star,3}\right) u_{\star,1} - u_{\star,2} = 0 \end{cases}$$

where $k_{\star,i} = k_i(x_{\star,3})$. On the other hand, the system (2) and (27)–(29) is usually operated by manipulating with the process input u so that the steady-state concentration of primary product $x_{\star,2}$ reaches the optimal solution $x_{\star,2}^{\mathrm{opt}}$. Hence the mathematical formulation of this statement leads to

$$\max_{u_\star} x_{\star,2}\Big(x_{\star,1}\big(x_{\star,3}, u_\star\big), x_{\star,3}, u_\star\Big) \tag{30}$$

subject to $x_{\star,1} > 0$ and $x_{\star,3}^{\min} \leq x_{\star,3} \leq x_{\star,3}^{\max}$

In (30), $x_{\star,3}^{\min}$ and $x_{\star,3}^{\max}$ are the physical bounds imposed on the temperature for practical implementation. This optimization problem is an implicit nonlinear programming one with constraints. The optimal solution can be found by analytical/numerical methods [45]. As an example, a simple solution to (30) (that is, $x_{\star,2}^{\mathrm{opt}} = 0.96$ (mol/l) corresponding to $x_{\star,1}^{\mathrm{opt}} = 1.87$ (mol/l) and $x_{\star,3}^{\mathrm{opt}} = 392.67$ (K) when $x_{\star,3}^{\min} = 382$ (K), $x_{\star,3}^{\max} = 407$ (K), $u_{\star,2} = -1100$ (kJ/(l.h)) and $u_{\star,1}$ fixed at 19.52 (1/h)) is found using the iterative algorithm. Physically, the cooling system needs to efficiently remove excess heat from the reaction process to drive the dynamics (2), (27) and (28) to the optimal equilibrium point. In what follows, $\boldsymbol{x}_\star^{\mathrm{opt}}$ will be used as the set-point, i.e $\boldsymbol{x}_{\star r} \triangleq \boldsymbol{x}_\star^{\mathrm{opt}}$, for the illustration of the control design.

3.1.3. The control design

First of all, we check quickly the isothermal case, thereby leading to the simplified vector field $f(\boldsymbol{x}) = \begin{bmatrix} -k_1 x_1 - 2k_3 x_1^2 \\ k_1 x_1 - k_2 x_2 \end{bmatrix}$

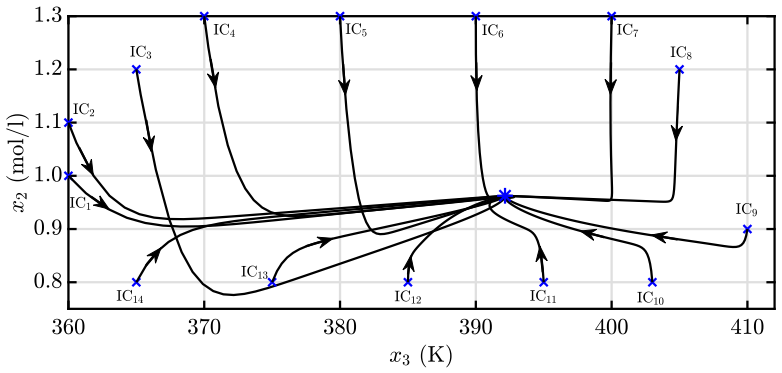

Fig. 2. The closed-loop phase plane.

from Eq. (27). The separability condition (3) follows immediately with $\mathcal{H}(\boldsymbol{x})$ (1) where $R_{di} = \text{diag}(1, 1)$ and $J(\boldsymbol{x}) = \begin{bmatrix} 0 & -k_1/2 \\ k_1/2 & 0 \end{bmatrix}$ and $R(\boldsymbol{x}) = \begin{bmatrix} k_1 + 2k_3x_1 & -k_1/2 \\ -k_1/2 & k_2 \end{bmatrix}$. Hence the resulting representation (4) is a non-relaxing EPH model ($\in \mathcal{H}_{e,nr}$) since all the principal minors determinants of $R(\boldsymbol{x})$ are positive (i.e., $R(\boldsymbol{x})$ is positive definite) due to the fact that $k_1 = k_2$. A feedback law, given by (24) with $\mathcal{I} = \{1\}$ or $\mathcal{I} = \{2\}$, therefore globally exponentially stabilizes the isothermal system at $\boldsymbol{x}_{\star r}$.

Unlike the isothermal case, the Hamiltonian formulation of the non-isothermal dynamics, associated with the unified quadratic storage function $\mathcal{H}(\boldsymbol{x})$ (1), can only be obtained with losing some structural properties due to the nonlinearities of thermal effects. Indeed, we reconsider a single-variable change given by [26] $\bar{x}_3 = -\frac{\rho C_p}{\Delta H_3}x_3$,[8] thereby leading to the alternative dynamics as $\dot{\bar{\boldsymbol{x}}} = f(\bar{\boldsymbol{x}}) + g(\bar{\boldsymbol{x}})u$ where $\bar{\boldsymbol{x}} = (x_1, x_2, \bar{x}_3)^\top \in \bar{\mathbb{D}}$ with $\bar{\mathbb{D}} = (0 \quad x_{10})^2 \times (-\infty \quad 0)$, u as seen in (28) and,

$$f(\bar{\boldsymbol{x}}) = \begin{bmatrix} -\bar{k}_1x_1 - 2\bar{k}_3x_1^2 \\ \bar{k}_1x_1 - \bar{k}_2x_2 \\ \frac{\Delta H_1\bar{k}_1x_1 + \Delta H_2\bar{k}_2x_2 + 2\Delta H_3\bar{k}_3x_1^2}{\Delta H_3} \end{bmatrix} \tag{31}$$

$$g(\bar{\boldsymbol{x}}) = \begin{bmatrix} x_{10} - x_1 & 0 \\ -x_2 & 0 \\ -\frac{\rho C_p}{\Delta H_3}\left(x_{30} + \frac{\Delta H_3}{\rho C_p}\bar{x}_3\right) & -\frac{1}{\Delta H_3} \end{bmatrix} \tag{32}$$

in which the term $\bar{k}_i \triangleq k_i(\bar{x}_3)$ has been used. Note that the equivalent set-point is $\bar{\boldsymbol{x}}_{\star r} \triangleq \bar{\boldsymbol{x}}_\star^{\text{opt}}$ with $\bar{\boldsymbol{x}}_\star^{\text{opt}} = (x_{\star,1}^{\text{opt}}, x_{\star,2}^{\text{opt}}, -\frac{\rho C_p}{\Delta H_3}x_{\star,3}^{\text{opt}})^\top$. We state the following proposition that corresponds to a specified version of Theorem 1.

Proposition 1. *The system dynamics expressed by $\bar{\boldsymbol{x}}$ admits an EPH presentation (i.e., $\in \mathcal{H}_{e,r}$) with the Hamiltonian storage function $\mathcal{H}(\bar{\boldsymbol{x}})$ given by (1) where $R_{di} = diag(1, 1, 1)$, and the structural matrices as below*

$$J(\bar{\boldsymbol{x}}) = \begin{bmatrix} 0 & a_1 & b_1 \\ -a_1 & 0 & 0 \\ -b_1 & 0 & 0 \end{bmatrix} \text{ and } R(\bar{\boldsymbol{x}}) = \begin{bmatrix} d_1 & e_1 & 0 \\ e_1 & d_2 & 0 \\ 0 & 0 & d_3 \end{bmatrix} \tag{33}$$

where $\bar{\boldsymbol{x}} \in \bar{\mathbb{D}}$; $a_1 = -\frac{\bar{k}_1}{2} + \frac{\bar{k}_3x_1\bar{x}_3}{x_2} + \frac{\Delta H_2}{\Delta H_3}\frac{\bar{k}_2\bar{x}_3}{2x_1}$; $b_1 = -2\bar{k}_3x_1 - \frac{\Delta H_2}{\Delta H_3}\frac{\bar{k}_2x_2}{x_1}$; $d_1 = \bar{k}_1 + 2\bar{k}_3x_1 > 0$; $d_2 = \bar{k}_2 > 0$; $d_3 = -\frac{\Delta H_1}{\Delta H_3}\frac{\bar{k}_1x_1}{\bar{x}_3} > 0$ and $e_1 = -\frac{\bar{k}_1}{2} - \frac{\bar{k}_3x_1\bar{x}_3}{x_2} - \frac{\Delta H_2}{\Delta H_3}\frac{\bar{k}_2\bar{x}_3}{2x_1}$. Consequently, a simple choice of the damping injection $R_l(\bar{\boldsymbol{x}})$

$$R_l(\bar{\boldsymbol{x}}) = diag(r_{1,l}, r_{2,l}, r_{3,l}) \tag{34}$$

where $r_{3,l} > 0$ and

$$r_{1,l} = \frac{\bar{k}_3x_1\bar{x}_3}{x_2} + \frac{\Delta H_2}{\Delta H_3}\frac{\bar{k}_2\bar{x}_3}{2x_1} + \alpha > 0 \tag{35}$$

$$r_{2,l} = 2\bar{k}_3x_1 + \frac{\bar{k}_3x_1\bar{x}_3}{x_2} + \frac{\Delta H_2}{\Delta H_3}\frac{\bar{k}_2\bar{x}_3}{2x_1} + \alpha > 0 \tag{36}$$

with $\alpha \in \mathbb{R}_+$ as an additional scalar guarantees the global asymptotic convergence of the dynamics of $\bar{\boldsymbol{x}}$ to $\bar{\boldsymbol{x}}_d$ with

$$\dot{\bar{\boldsymbol{x}}}_d \triangleq \left[J(\bar{\boldsymbol{x}}) - R(\bar{\boldsymbol{x}})\right]\frac{\partial\mathcal{H}(\bar{\boldsymbol{x}}_d)}{\partial\bar{\boldsymbol{x}}_d} + R_l(\bar{\boldsymbol{x}})\frac{\partial\mathscr{H}(\bar{\boldsymbol{e}}_r)}{\partial\bar{\boldsymbol{e}}_r} + g(\bar{\boldsymbol{x}})u \tag{37}$$

where $\bar{\boldsymbol{e}}_r = \bar{\boldsymbol{x}} - \bar{\boldsymbol{x}}_d$ while u and $g(\bar{\boldsymbol{x}})$ are given in (28) and (32), respectively.

Proof. First one derives using (31) $f(\bar{\boldsymbol{x}}) = M(\bar{\boldsymbol{x}})\frac{\partial\mathcal{H}(\bar{\boldsymbol{x}})}{\partial\bar{\boldsymbol{x}}}$ with

$$M(\bar{\boldsymbol{x}}) = \begin{bmatrix} -d_1 & a_1 - e_1 & b_1 \\ -a_1 - e_1 & -d_2 & 0 \\ -b_1 & 0 & -d_3 \end{bmatrix}$$

and $\frac{\partial\mathcal{H}(\bar{\boldsymbol{x}})}{\partial\bar{\boldsymbol{x}}} = (x_1, x_2, \bar{x}_3)^\top$. From this, $J(\bar{\boldsymbol{x}})$ and $R(\bar{\boldsymbol{x}})$ are shown as seen in (33) by considering $J(\bar{\boldsymbol{x}}) = \frac{M(\bar{\boldsymbol{x}}) - M(\bar{\boldsymbol{x}})^\top}{2}$ and $R(\bar{\boldsymbol{x}}) = -\frac{M(\bar{\boldsymbol{x}}) + M(\bar{\boldsymbol{x}})^\top}{2}$, respectively. It is worth noting that $\frac{\Delta H_1}{\Delta H_3} < 0$ and $\frac{\Delta H_2}{\Delta H_3} > 0$. The first part of the proof follows immediately. In other words, the symmetric matrix $R(\bar{\boldsymbol{x}}) + R_l(\bar{\boldsymbol{x}})$ is positive definite thanks to the Schur complement lemma since all its principal minors determinants given by $\Delta_1 = d_1 + r_{1,l}$, $\Delta_2 = (d_1 + r_{1,l})(d_2 + r_{2,l}) - e_1^2$ and $\Delta_3 = (d_3 + r_{3,l})\Delta_2$ are positive. Finally we can check easily that one of the following two selections, $\mathcal{I} = \{1, 3\}$ yielding $g_s(\bar{\boldsymbol{x}}) = \begin{bmatrix} x_{10} - x_1 & 0 \\ -\frac{\rho C_p}{\Delta H_3}\left(x_{30} + \frac{\Delta H_3}{\rho C_p}\bar{x}_3\right) & -\frac{1}{\Delta H_3} \end{bmatrix}$ or $\mathcal{I} = \{2, 3\}$ yielding $g_s(\bar{\boldsymbol{x}}) = \begin{bmatrix} -x_2 & 0 \\ -\frac{\rho C_p}{\Delta H_3}\left(x_{30} + \frac{\Delta H_3}{\rho C_p}\bar{x}_3\right) & -\frac{1}{\Delta H_3} \end{bmatrix}$, can be adopted and for that Assumption 2 holds. The latter concludes the proof by invoking Theorem 1 to compute the feedback law for u where we adapt the notations $\boldsymbol{x}$ with $\bar{\boldsymbol{x}}$, and $\boldsymbol{x}_d$ with $\bar{\boldsymbol{x}}_d$ while designating $(\bar{\boldsymbol{x}}_d)_\mathcal{I}$. ■

For the sake of illustration, the feasible subset $\mathcal{I} = \{2, 3\}$ is considered to derive the control equation for $u = [u_1 \quad u_2]^\top$ (28)

[8] It should be noted that this change of variable does not constitute and is different from the nonlinear canonical transformation via solving a PDE [17] and/or the linear time-invariant state transformation that is constructed from the stoichiometry [29]. The advantage of using this new notation is to express the resulting dynamics in terms of the dimensionless parameters $\frac{\Delta H_1}{\Delta H_3} < 0$ and $\frac{\Delta H_2}{\Delta H_3} > 0$, and therefore enables the quadratic EPH formulation and control design.

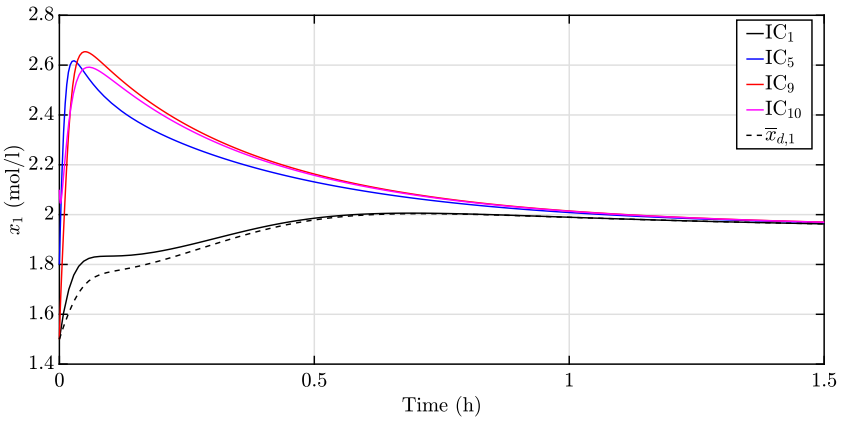

(a) x_1

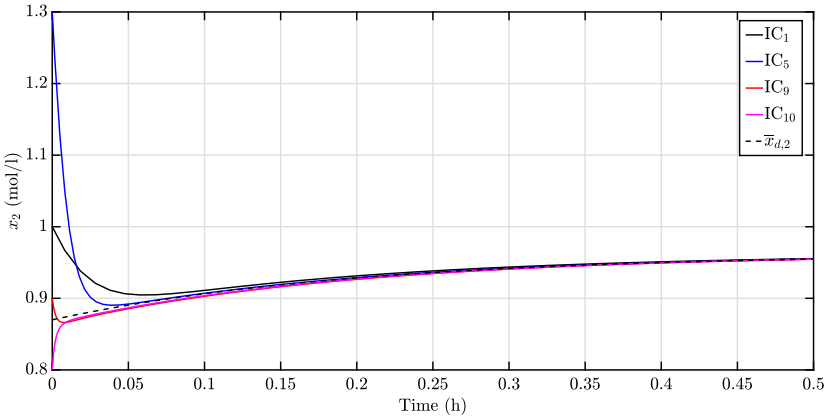

(b) x_2

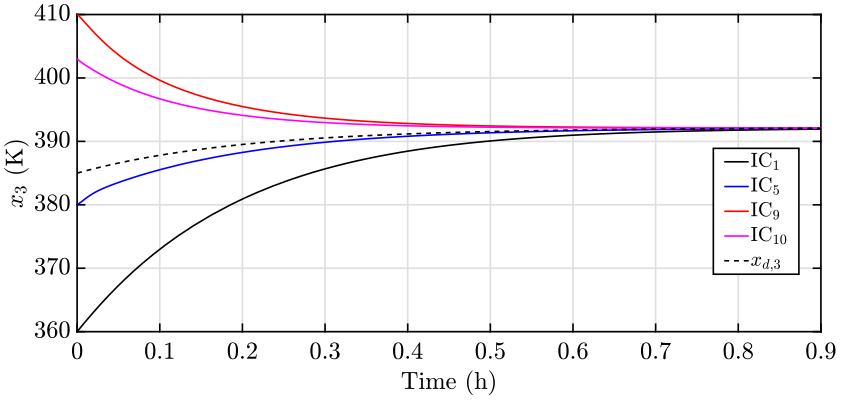

(c) x_3

Fig. 3. The dynamics of x_1, x_2 and x_3 with several representative initial conditions.

using (24) with $g_s(\bar{\boldsymbol{x}})^{-1} = \begin{bmatrix} -\frac{1}{x_2} & 0 \\ \frac{\rho C_p}{x_2}\left(x_{30} + \frac{\Delta H_3}{\rho C_p}\bar{x}_3\right) & -\Delta H_3 \end{bmatrix}$ and $K_{\text{di,I}}$ and $K_{\text{di,P}}$ being zero matrices as follows:

$$u_1 = -\frac{1}{x_2}\left(\dot{\bar{x}}_{d,2} - \bar{k}_1\bar{x}_{d,1} + \bar{k}_2\bar{x}_{d,2} - r_{2,I}(x_2 - \bar{x}_{d,2})\right), \tag{38}$$

$$\begin{aligned} u_2 = &-\Delta H_3\Bigg[\dot{\bar{x}}_{d,3} - \left(2\bar{k}_3x_1 + \frac{\Delta H_2}{\Delta H_3}\frac{\bar{k}_2x_2}{x_1}\right)\bar{x}_{d,1} \\ &- \frac{\Delta H_1}{\Delta H_3}\frac{\bar{k}_1x_1}{\bar{x}_3}\bar{x}_{d,3} - r_{3,I}(\bar{x}_3 - \bar{x}_{d,3})\Bigg] \\ &+ \frac{\rho C_p}{x_2}\left(x_{30} + \frac{\Delta H_3}{\rho C_p}\bar{x}_3\right) \\ &\times \left(\dot{\bar{x}}_{d,2} - \bar{k}_1\bar{x}_{d,1} + \bar{k}_2\bar{x}_{d,2} - r_{2,I}(x_2 - \bar{x}_{d,2})\right), \end{aligned} \tag{39}$$

where $\dot{\bar{x}}_{d,i}$ is assigned as analogous to (21) with $\kappa_i = 5$, $\gamma_i =$

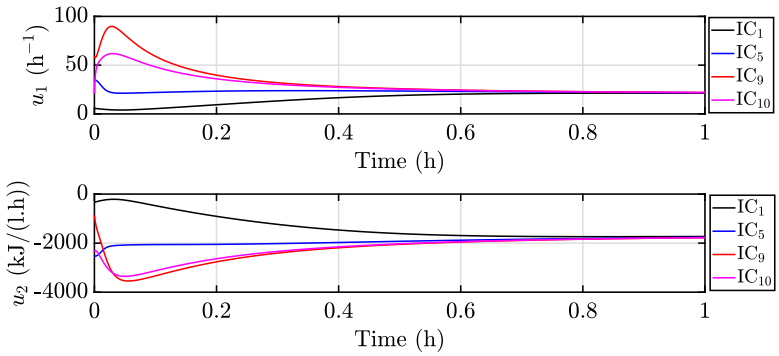

Fig. 4. The dynamics of the control inputs with several representative initial conditions.

1, $i \in \mathcal{I}$, and $\bar{x}_{d,1}$ is constructed from the integration of $\dot{\bar{x}}_{d,1}$ given by (13)

$$\begin{aligned}\dot{\bar{x}}_{d,1} = &-\left(\bar{k}_1 + 2k_3x_1\right)\bar{x}_{d,1} + \left(\frac{2\bar{k}_3x_1\bar{x}_3}{x_2} + \frac{\Delta H_2}{\Delta H_3}\frac{\bar{k}_2\bar{x}_3}{x_1}\right)\bar{x}_{d,2}\\ &- \left(2\bar{k}_3x_1 + \frac{\Delta H_2}{\Delta H_3}\frac{\bar{k}_2x_2}{x_1}\right)\bar{x}_{d,3}\\ &+ r_{1,I}(x_1 - \bar{x}_{d,1})\\ &- \frac{(x_{10} - x_1)}{x_2}\left(\dot{\bar{x}}_{d,2} - \bar{k}_1\bar{x}_{d,1} + \bar{k}_2\bar{x}_{d,2} - r_{2,I}(x_2 - \bar{x}_{d,2})\right).\end{aligned} \tag{40}$$

Additionally, $R_I(\bar{\boldsymbol{x}})$ is computed using $\alpha = 15$ and $r_{3,I} = 5$. Obviously, the control inputs u_1 (38) and u_2 (39) as well as $\dot{\bar{x}}_{d,1}$ (40) are well-defined because x_1, x_2 and $\bar{x}_3$ never equal zero. Fig. 2 shows that the trajectories x_2 and x_3 converge to the desired steady states $x^{\text{opt}}_{\star,2}$ and $x^{\text{opt}}_{\star,3}$, respectively, from fourteen initial conditions lying everywhere in the phase plane (denoted by IC$_1$, IC$_2$, ..., IC$_{14}$; we refer also to Appendix B for their values). This means that the system state reaches the optimal equilibrium point $\boldsymbol{x}^{\text{opt}}_{\star}$. Moreover, it can be clearly seen from Fig. 3 that the dynamics of x_1, x_2 and x_3 starting from several representative initial conditions converge to the corresponding reference trajectories $x_{d,1}$ $(= \bar{x}_{d,1})$, $x_{d,2}$ $(= \bar{x}_{d,2})$ and $x_{d,3}$ $\left(= -\frac{\Delta H_3}{\rho C_p}\bar{x}_{d,3}\right)$ passing through $x^{\text{opt}}_{\star,1}$, $x^{\text{opt}}_{\star,2}$ and $x^{\text{opt}}_{\star,3}$, respectively. It, therefore, supports the theoretical developments in Proposition 1 (also Theorem 1). In addition, Fig. 4 shows the time evolution of the control inputs including u_1 and u_2. Note that the proposed enhanced TEBC approach can also be applied to the system at hand with single input scenario being either u_1 or u_2 by considering $\mathcal{I} = \{3\}$, $g(\boldsymbol{x}) = [g_1(\boldsymbol{x}) \quad g_2(\boldsymbol{x})]$ and splitting $g(\boldsymbol{x})u$ (28) into $g_1(\boldsymbol{x})u_1 + g_2(\boldsymbol{x})u_2$.

Furthermore, the proposed TEBC approach with the PI action (25) in (24) can improve the robustness of the closed-loop system against the model uncertainty. For example, we assume that the density of the mixture is uncertain[9] and proportional to the nominal value as $\rho' = 1.1\rho$ (i.e. an error of 10%). In that respect, the matrices $K_{\text{di,P}} = \begin{bmatrix}250 & 4962.7\\ 4962.7 & 98515\end{bmatrix}$ and $K_{\text{di,I}} = \begin{bmatrix}275 & 0\\ 0 & 470\end{bmatrix}$ are chosen. It can be clearly seen from Fig. 5 that the state variables under the PI-TEBC converge to the desired setpoints after a settling time $t_s = 1.2$ hours while the normal TEBC needs to be re-tuned with $r_{3,I} = 90$ to guarantee the convergence of x_1, x_2 and x_3 in the same period. Obviously, fine oscillations in the x_1 and x_2 dynamics confirm the presence of the integral action. On the other hand, as shown in Fig. 6, under the PI-TEBC, the dynamics and amplitude of the manipulated variables are physically admissible. Note, however, that under the re-tuned TEBC a large and sudden variation of u_2 from -1000 to -5000 kJ/(l.h) is needed at the beginning of the reaction course to cool down (and thus to stabilize) the reactor, which may be impractical.

3.2. Case study 2: A mechanical system without equilibrium

3.2.1. Model description

In this section, we illustrate the proposed method via the tracking control of 3−DOF SCARA Robot toward a reference trajectory without equilibrium. The dynamics of the robot can be expressed by (2) [47,48] in terms of the state $\boldsymbol{x} = \left(\boldsymbol{q}^\top, \boldsymbol{v}^\top\right)^\top$ with $\boldsymbol{q} = (\theta_1, \theta_2, z)^\top$ being the position vector, $\boldsymbol{v} = (v_1, v_2, v_z)^\top$ being the velocity vector and

$$f(\boldsymbol{x}) = \begin{bmatrix}\boldsymbol{v}\\ -\mathcal{M}(\boldsymbol{q})^{-1}\left(\frac{\partial P(\boldsymbol{q})}{\partial \boldsymbol{q}} + D\boldsymbol{v}\right)\end{bmatrix}, \quad g(\boldsymbol{x}) = \begin{pmatrix}\mathbf{0}_3\\ \mathcal{M}^{-1}(\boldsymbol{q})\end{pmatrix} \quad \text{and} \quad u = \begin{pmatrix}u_{m,1}\\ u_{m,2}\\ u_z\end{pmatrix}. \tag{41}$$

For the sake of brevity and clarity, we refer the reader to [47,48] for more details on the notations used. In this model, $\mathcal{M}(\boldsymbol{q}) = \begin{bmatrix}\mathcal{M}_{11} & \mathcal{M}_{12} & 0\\ \mathcal{M}_{12} & m_3l_2^2 & 0\\ 0 & 0 & (m_1+m_2+m_3)\mathrm{g}\end{bmatrix}$ (with $\mathcal{M}_{11} = (m_2+m_3)l_1^2 + m_3l_2^2 + 2m_3l_1l_2\cos(\theta_2)$ and $\mathcal{M}_{12} = m_3l_2^2 + m_3l_1l_2\cos(\theta_2)$) is the positive-definite inertia matrix, $P(\boldsymbol{q}) = (m_1+m_2+m_3)\mathrm{g}z$ is the total potential energy and $D = \mathrm{diag}(D_1, D_2, D_3) > 0$ is the natural damping matrix and u is the control input force vector. Additionally, $\mathbf{0}_3$ denotes the 3×3 zero matrix. Numerical values of the physical parameters are listed in Appendix C.

3.2.2. The control design

To formulate the robot dynamics into the EPH representation with $\mathcal{H}(\boldsymbol{x})$ (1), we consider a single-variable change of u_z as $u'_z = u_z - (m_1+m_2+m_3)\mathrm{g}$ that leads to an alternative dynamics of $\boldsymbol{x}$ as follows $\dot{\boldsymbol{x}} = f'(\boldsymbol{x}) + g(\boldsymbol{x})u'$, where $g(\boldsymbol{x})$ is same as (41) while $u' = \begin{pmatrix}u_{m,1} & u_{m,2} & u'_z\end{pmatrix}^\top$ and $f'(\boldsymbol{x}) = \begin{bmatrix}\boldsymbol{v}\\ -\mathcal{M}(\boldsymbol{q})^{-1}D\boldsymbol{v}\end{bmatrix}$ are given. We state the following proposition that corresponds to a specified version of Theorem 1.

[9] In practice, kinetic model is not easy to obtain and almost assumed to be known for the computation and design purposes. Otherwise, we refer the reader to [46] for a detailed analysis.

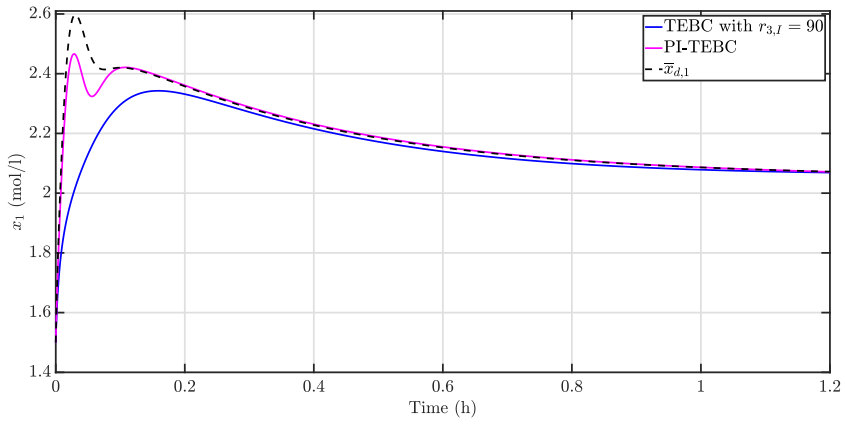

(a) x_1

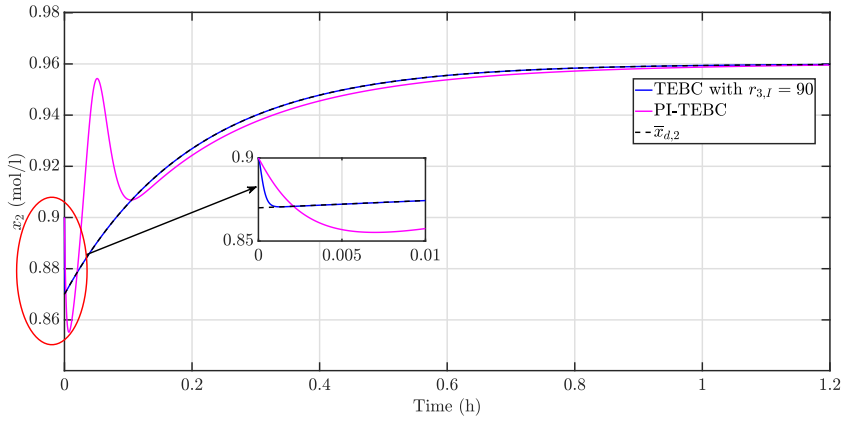

(b) x_2

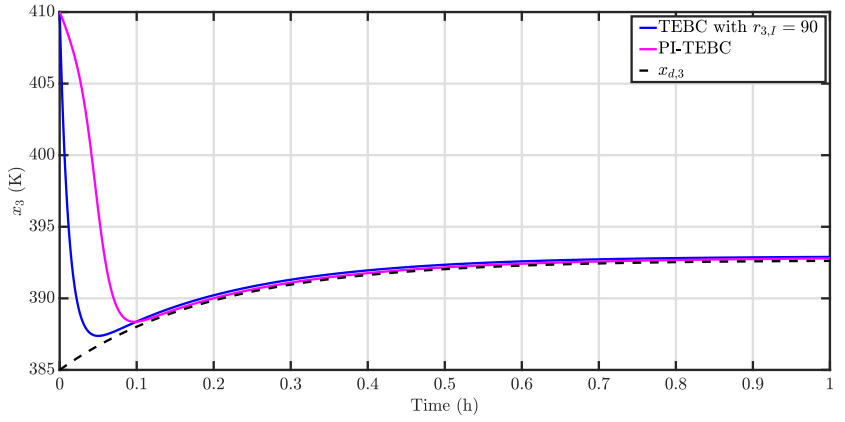

(c) x_3

Fig. 5. The dynamics of x_1, x_2 and x_3 for IC_9 with the uncertain density.

Proposition 2. *The robot dynamics described by* $\dot{\boldsymbol{x}} = f'(\boldsymbol{x}) + g(\boldsymbol{x})u'$ *can be formulated into an EPH representation, i.e.* $\in \mathcal{H}_{e,r}$, *with the storage function* $\mathcal{H}(\boldsymbol{x})$ (1) *and the following structural matrices*

$$J(\boldsymbol{x}) = \frac{1}{2}\begin{pmatrix} \mathbf{0}_3 & \mathbf{I}_3 \\ -\mathbf{I}_3 & \mathbf{0}_3 \end{pmatrix} \quad \text{and} \quad R(\boldsymbol{x}) = \frac{-1}{2}\begin{pmatrix} \mathbf{0}_3 & \mathbf{I}_3 \\ \mathbf{I}_3 & -2\mathcal{M}(\boldsymbol{q})^{-1}D \end{pmatrix}, \tag{42}$$

where $\mathbf{I}_3$ *denotes the identity matrix and* $\mathcal{M}(\boldsymbol{q})^{-1}$ *is given by*

$$\mathcal{M}(\boldsymbol{q})^{-1} = \begin{bmatrix} \frac{m_3 l_2^2}{\mathrm{D}_{\mathcal{M}}} & \frac{-\mathcal{M}_{12}}{\mathrm{D}_{\mathcal{M}}} & 0 \\ \frac{-\mathcal{M}_{12}}{\mathrm{D}_{\mathcal{M}}} & \frac{\mathcal{M}_{11}}{\mathrm{D}_{\mathcal{M}}} & 0 \\ 0 & 0 & \frac{1}{(m_1+m_2+m_3)\mathrm{g}} \end{bmatrix} \tag{43}$$

with $\mathrm{D}_{\mathcal{M}} = \mathcal{M}_{11} m_3 l_2^2 - \mathcal{M}_{12}^2 > 0$.

In addition, if the damping injection $R_I = diag(R_{I,1}, R_{I,2})$ *(with* $R_{I,1} = diag(r_{I,1}, r_{I,2}, r_{I,3})$ *and* $R_{I,2} = diag(r_{I,4}, r_{I,5}, r_{I,6})$*) is chosen as* $R_{I,1} > 0$, $r_{I,4} = \frac{1}{4r_{I,1}} + \alpha_1$, $r_{I,5} = \frac{1}{4r_{I,2}} + \alpha_2$ *and* $r_{I,6} = \frac{1}{4r_{I,3}} +$

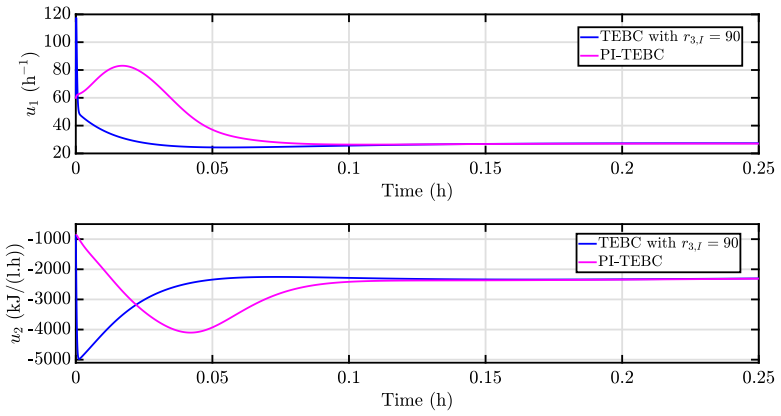

Fig. 6. The representation of control inputs for IC_9 with the uncertain density.

$$\mathcal{R}(\boldsymbol{x}) = \begin{bmatrix} r_{I,1}\left(r_{I,4} + \frac{m_3 l_2^2 D_1}{\mathrm{D}_{\mathcal{M}}}\right) - \frac{1}{4} & -r_{I,1}\frac{\mathcal{M}_{12}D_1}{\mathrm{D}_{\mathcal{M}}} & 0 \\ -r_{I,2}\frac{\mathcal{M}_{12}D_2}{\mathrm{D}_{\mathcal{M}}} & r_{I,2}\left(r_{I,5} + \frac{\mathcal{M}_{11}D_2}{\mathrm{D}_{\mathcal{M}}}\right) - \frac{1}{4} & 0 \\ 0 & 0 & r_{I,3}\left[r_{I,6} + \frac{D_3}{(m_1+m_2+m_3)\mathrm{g}}\right] - \frac{1}{4} \end{bmatrix},$$

Box I.

$\alpha_3,\ \alpha_1, \alpha_2, \alpha_3 \in \mathbb{R}_+$, *then* $\boldsymbol{x}$ *asymptotically tracks* $\boldsymbol{x}_d = \left(\boldsymbol{q}_d^\top, \boldsymbol{v}_d^\top\right)^\top$ *(with* $\boldsymbol{q}_d = \left(\theta_{d,1}, \theta_{d,2}, z_d\right)^\top$ *and* $\boldsymbol{v}_d = \left(v_{d,1}, v_{d,2}, v_{d,z}\right)^\top$*) where the reference dynamics is of the form*

$$\dot{\boldsymbol{x}}_d = [J(\boldsymbol{x}) - R(\boldsymbol{x})]\frac{\partial \mathcal{H}(\boldsymbol{x}_d)}{\partial \boldsymbol{x}_d} + R_I \frac{\partial \mathscr{K}(\boldsymbol{e}_r)}{\partial \boldsymbol{e}_r} + g(\boldsymbol{x})u'. \tag{44}$$

Proof. It can be seen from (41) that $f(\boldsymbol{x})$ can be separated as $f(\boldsymbol{x}) = Q(\boldsymbol{x})\frac{\partial \mathcal{H}(\boldsymbol{x})}{\partial \boldsymbol{x}}$ with $Q(\boldsymbol{x}) = \begin{bmatrix} \mathbf{0}_3 & \mathbf{I}_3 \\ \mathbf{0}_3 & -\mathcal{M}(\boldsymbol{q})^{-1}D \end{bmatrix}$, thereby leading to the expressions of $J(\boldsymbol{x})$ and $R(\boldsymbol{x})$ as shown in (42) by employing $J(\boldsymbol{x}) = \frac{Q(\boldsymbol{x}) - Q(\boldsymbol{x})^\top}{2}$ and $R(\boldsymbol{x}) = -\frac{Q(\boldsymbol{x}) + Q(\boldsymbol{x})^\top}{2}$. Hence, the first part of this proof then follows immediately.

On the other hand, we can easily check that the condition (11), i.e. $R(\boldsymbol{x}) + R_I > 0$, is met if the matrix $\mathcal{R}(\boldsymbol{x}) \triangleq R_{I,1}\left[R_{I,2} + \mathcal{M}(\boldsymbol{q})^{-1}D\right] - \frac{\mathbf{I}_3}{4}$ is positive definite. As the explicit form of $\mathcal{R}(\boldsymbol{x})$ is given in Box I, its principal minors determinants are thus obtained as

$$\Delta_1 = r_{I,1}\left(r_{I,4} + \frac{m_3 l_2^2 D_1}{\mathrm{D}_{\mathcal{M}}}\right) - \frac{1}{4} > 0, \tag{45}$$

$$\begin{aligned}\Delta_2 =& \left[r_{I,1}\left(r_{I,4} + \frac{m_3 l_2^2 D_1}{\mathrm{D}_{\mathcal{M}}}\right) - \frac{1}{4}\right]\left[r_{I,2}\left(r_{I,5} + \frac{\mathcal{M}_{11}D_2}{\mathrm{D}_{\mathcal{M}}}\right) - \frac{1}{4}\right] \\ &- r_{I,1}r_{I,2}D_1D_2\left(\frac{\mathcal{M}_{12}}{\mathrm{D}_{\mathcal{M}}}\right)^2 \\ =& r_{I,2}\frac{\mathcal{M}_{11}D_2}{\mathrm{D}_{\mathcal{M}}}\left(r_{I,1}r_{I,4} - \frac{1}{4}\right) + r_{I,1}\frac{m_3 l_2^2 D_1}{\mathrm{D}_{\mathcal{M}}}\left(r_{I,2}r_{I,5} - \frac{1}{4}\right) + \\ &\left(r_{I,1}r_{I,4} - \frac{1}{4}\right)\left(r_{I,2}r_{I,5} - \frac{1}{4}\right) \\ &+ r_{I,1}r_{I,2}\frac{D_1D_2}{\mathrm{D}_{\mathcal{M}}^2}\left(m_3 l_2^2 \mathcal{M}_{11} - \mathcal{M}_{12}^2\right) > 0, \end{aligned} \tag{46}$$

$$\Delta_3 = \left\{r_{I,3}\left[r_{I,6} + \frac{D_3}{(m_1+m_2+m_3)\mathrm{g}}\right] - \frac{1}{4}\right\}\Delta_2 > 0, \tag{47}$$

which are positive due to $\mathcal{M}(\boldsymbol{q}) > 0$. Hence the positive definite property of $\mathcal{R}(\boldsymbol{x})$ immediately follows using Schur complement lemma.

Finally, a selection $\mathcal{I} = \{4, 5, 6\}$ is made leading to $g_s(\boldsymbol{x}) = \mathcal{M}(\boldsymbol{q})^{-1}$ given by (43). Note, in this case, that $(\boldsymbol{x})_{\mathcal{I}}$ $(= \boldsymbol{v})$ and the position vector $\boldsymbol{q}$ can be determined by the integration of the velocity vector $\boldsymbol{v}$ over time. We complete the proof by invoking Theorem 1 with the adaptation of u by u' to compute the feedback law while designating $(\boldsymbol{x}_d)_{\mathcal{I}}$. ■

For the sake of illustration, $R_{I,1} = \mathrm{diag}(1, 1, 1)$, $\alpha_1 = 29.75$, $\alpha_2 = 49.75$ and $\alpha_3 = 1.75$ are chosen, whereas $K_{\mathrm{di,P}}$ and $K_{\mathrm{di,I}}$ are zero matrices (i.e. without the PI action for simplicity and due to space limitations). And, $(\boldsymbol{x}_d)_{\mathcal{I}}$, i.e. $\boldsymbol{v}_d$, is assigned directly as $\boldsymbol{v}_d = [\cos(t) \quad -\sin(\frac{\pi}{2} - t) \quad \cos(t)]^\top$ whereas $(\boldsymbol{x}_d)_{\mathcal{J}}$, i.e. $\boldsymbol{q}_d = \left(\theta_{d,1}, \theta_{d,2}, z_d\right)^\top$, is then constructed from the integration of $\dot{\theta}_{d,1}$, $\dot{\theta}_{d,2}$ and $\dot{z}_d$ which are respectively given by $\dot{\theta}_{d,1} = v_{d,1} + r_{I,1}(\theta_1 - \theta_{d,1})$, $\dot{\theta}_{d,2} = v_{d,2} + r_{I,2}(\theta_2 - \theta_{d,2})$ and $\dot{z}_d = v_{d,z} + r_{I,3}(z - z_d)$ using (13). Consequently, the control inputs $u_{m,1}$, $u_{m,2}$ and u_z' expressed by

$$\begin{bmatrix} u_{m,1} \\ u_{m,2} \\ u_z' \end{bmatrix} = \mathcal{M}(\boldsymbol{q})\begin{bmatrix} \dot{v}_{d,1} + \frac{m_3 l_2^2}{\mathrm{D}_{\mathcal{M}}}D_1 v_{d,1} - \frac{\mathcal{M}_{12}}{\mathrm{D}_{\mathcal{M}}}D_2 v_{d,2} - r_{I,4}(v_1 - v_{d,1}) \\ \dot{v}_{d,2} - \frac{\mathcal{M}_{12}}{\mathrm{D}_{\mathcal{M}}}D_1 v_{d,1} + \frac{\mathcal{M}_{11}}{\mathrm{D}_{\mathcal{M}}}D_2 v_{d,2} - r_{I,5}(v_2 - v_{d,2}) \\ \dot{v}_{d,z} + \frac{D_3}{(m_1+m_2+m_3)\mathrm{g}}v_{d,z} - r_{I,6}(v_z - v_{d,z}) \end{bmatrix} \tag{48}$$

are well-defined because of $\mathrm{D}_{\mathcal{M}} > 0$ and $\mathrm{g} \neq 0$. As shown in Fig. 7, the state variables v_1, v_2 and v_z track the desired reference states $v_{d,1}$, $v_{d,2}$ and $v_{d,z}$, respectively. In addition, θ_1, θ_2 and z track the generated corresponding reference states $\theta_{d,1}, \theta_{d,2}$ and z_d as seen in Fig. 8. Finally, Fig. 9 represents the time evolution of the control input forces $u_{m,1}$, $u_{m,2}$ and u_z.

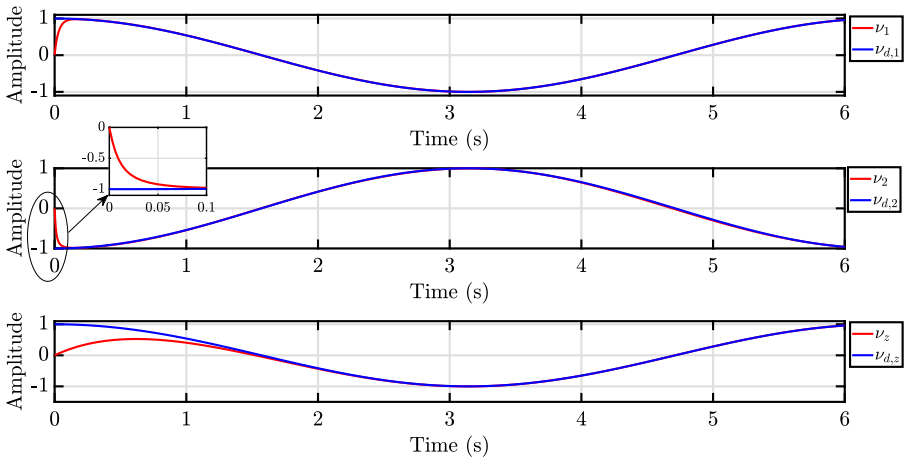

Fig. 7. The dynamics of $\boldsymbol{\nu}$.

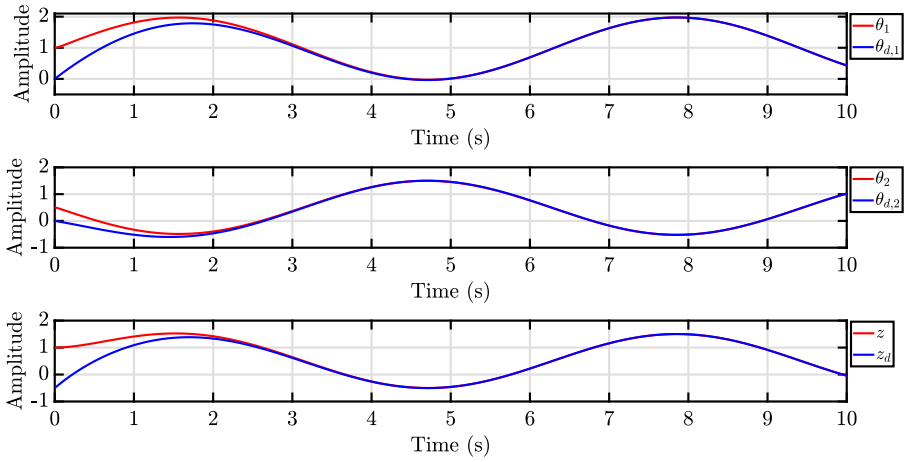

Fig. 8. The dynamics of $\boldsymbol{q}$.

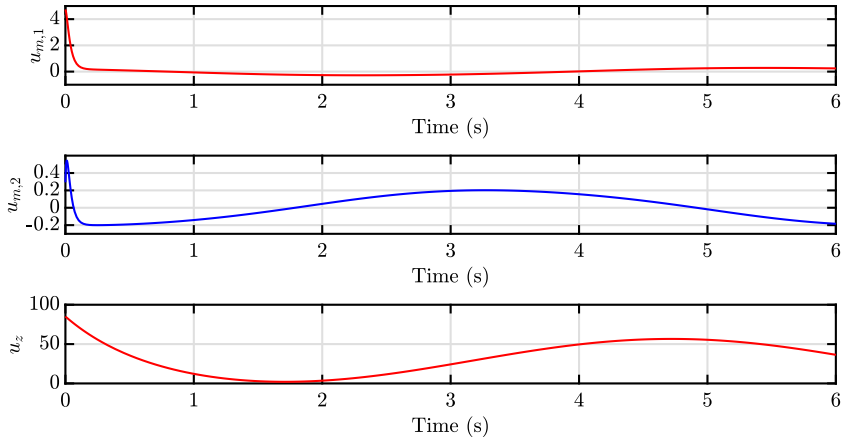

Fig. 9. The representation of control inputs.

4. Conclusion

In this work, an enhanced tracking-error-based control approach is developed for the control design of extended port-Hamiltonian systems (including possibly the pseudo port-Hamiltonian models) which are explicitly associated with a unified quadratic Hamiltonian storage function as similar as possible to that of electrical, mechanical, or electromechanical systems. The proposed approach guarantees the global asymptotic or exponential convergence of the system states to the reference states, while part of the reference states is directly assigned or chosen to achieve either finite-time or exponential/asymptotic stability. Besides, a Proportional–Integral action can also be added to the developed tracking controller for improving the closed-loop performance and robustness against the model uncertainty. One of the main computational advantages of the approach is that

input and/or state coordinate transformations are not involved in the control design as compared to [13,14,17], thereby decreasing the computational cost, while stabilizing a non-minimum phase nonlinear chemical system at a desired set-point with different convergence properties. Also, the proposed tracking control approach has also been applied to a 3-DOF SCARA robot without equilibrium.

Unlike the previous passivity-based control approaches applied to systems with equilibrium such as energy balancing passivity-based control, and interconnection and damping assignment passivity-based control [7,49] where their applications to the control design require to solve a set of PDEs or the approaches may make the control system worse whenever the dissipation obstacle occurs. As shown, the proposed enhanced TEBC approach seems efficient and flexible since the approach works out despite the aforementioned challenges. In that respect, an in-depth comparative analysis of these control approaches will be part of our future work.

CRediT authorship contribution statement

N.H. Hoang: Conceptualization, Methodology, Validation, Formal analysis, Writing – original draft, Writing – review & editing, Funding acquisition. **T.S. Nguyen:** Methodology, Formal analysis, Software, Writing – review & editing. **T.K.P. Le:** Methodology, Validation, Writing – review & editing. **T.T.H. Phan:** Methodology, Validation, Writing – review & editing. **M.A. Hussain:** Writing – review & editing. **D. Dochain:** Writing – review & editing.

Declaration of competing interest

The authors declare that they have no known competing financial interests or personal relationships that could have appeared to influence the work reported in this paper.

Acknowledgments

This research is funded by Vietnam National Foundation for Science and Technology Development (NAFOSTED) under grant number 103.99-2019.385.

Appendix A. Nomenclature and numerical values of the reaction system

All the numerical values here are extracted from [26], and references therein.

Symbol	Quantity/Value (Unit)
x_1, x_2	Molar concentrations of A and B, mol/l
x_3	Reactor temperature, K
u_1, u_2	Dilution rate, 1/h and heat removal rate, kJ/(l h)
x_{10}	Molar concentration of A in the inlet, mol/l $x_{10} = 5$
x_{30}	Reactor feed temperature, K $x_{30} = 403.15$
ρ	Density of reacting mixture, kg/l $\rho = 0.930$
C_p	Heat capacity of reacting mixture, kJ/(kg K) $C_p = 3.01$
ΔH_i	Heat of ith reaction, kJ/mol $\Delta H_1 = 4.20$; $\Delta H_2 = -11.00$ $\Delta H_3 = -41.85$
k_{i0}	Kinetic constant of ith reaction $k_{10}\left(= k_{20}\right) = 1.287 \times 10^{12}$ (1/h) $k_{30} = 9.403 \times 10^{9}$ (l/(mol h))
$\frac{E_i}{R}$	Activation temperature of ith reaction, K $\frac{E_1}{R}\left(= \frac{E_2}{R}\right) = 9758.3$; $\frac{E_3}{R} = 8560.0$

Appendix B. The initial conditions

All the initial conditions considered for the simulations are $IC_1 = (1.5, 1.0, 360)$; $IC_2 = (1.5, 1.1, 360)$; $IC_3 = (1.6, 1.2, 365)$; $IC_4 = (1.7, 1.3, 370)$; $IC_5 = (1.8, 1.3, 380)$; $IC_6 = (1.9, 1.3, 390)$; $IC_7 = (2.0, 1.3, 400)$; $IC_8 = (1.8, 1.2, 405)$; $IC_9 = (1.5, 0.9, 410)$; $IC_{10} = (2.1, 0.8, 403)$; $IC_{11} = (1.9, 0.8, 395)$; $IC_{12} = (1.8, 0.8, 385)$; $IC_{13} = (2.0, 0.8, 375)$ and $IC_{14} = (2.2, 0.8, 365)$.

Appendix C. Physical parameter values for 3-DOF SCARA robot

All the numerical values here are extracted from [47,48], and references therein.

Symbol	Value (Unit)	Symbol	Value (Unit)
m_1	1.510 (kg)	l_1	0.343 (m)
m_2	0.873 (kg)	l_2	0.267 (m)
m_3	0.500 (kg)	g	9.81 (m/s^2)

References

[1] S.H. Strogatz, Nonlinear Dynamics and Chaos: with Applications to Physics, Biology, Chemistry, and Engineering, second ed., CRC Press, Boca Raton, 2015, http://dx.doi.org/10.1201/9780429492563.
[2] P. Glansdorff, I. Prigogine, Thermodynamic Theory of Structure, Stability and Fluctuations, Wiley-Interscience, New York, 1971.
[3] K.J. Åström, R.M. Murray, Feedback Systems: An Introduction for Scientists and Engineers, Princeton University Press, Princeton, NJ, ISBN: 978-0-691-13576-2, 2008.
[4] D.Q. Mayne, Model predictive control: Recent developments and future promise, Automatica 50 (12) (2014) 2967–2986.
[5] M. Guay, D. Dochain, A time-varying extremum-seeking control approach, Automatica 51 (2015) 356–363.
[6] A. Van der Schaft, L_2-Gain and Passivity Techniques in Nonlinear Control, third ed., Springer, 2017.
[7] R. Ortega, A. Van der Schaft, I. Mareels, B. Maschke, Putting energy back in control, IEEE Control Syst. Mag. 21 (2) (2001) 18–33.
[8] R. Ortega, D. Jeltsema, J.M.A. Scherpen, Power shaping: A new paradigm for stabilization of nonlinear *RLC* circuits, IEEE Trans. on Autom. Control 48 (10) (2003) 1762–1767.
[9] A.A. Alonso, B.E. Ydstie, Stabilization of distributed systems using irreversible thermodynamics, Automatica 37 (11) (2001) 1739–1755.
[10] H. Ramírez, Y. Le Gorrec, B. Maschke, F. Couenne, On the passivity based control of irreversible processes: A port-Hamiltonian approach, Automatica 64 (2016) 105–111.
[11] A. Isidori, Nonlinear Control Systems, third ed., Springer-Verlag, London, 2013.
[12] H.K. Khalil, Nonlinear Systems, third ed., Prentice Hall, Upper Saddle River, 2002.
[13] C.I. Byrnes, A. Isidori, J.C. Willems, Passivity, feedback equivalence, and the global stabilization of minimum phase nonlinear systems, IEEE Trans. Autom. Control 36 (11) (1991) 1228–1240.
[14] M. Larsen, M. Janković, P.V. Kokotović, Coordinated passivation designs, Automatica 39 (2) (2003) 335–341.
[15] H. Sira-Ramírez, I. Angulo-Núnez, Passivity-based control of nonlinear chemical processes, Int. J. Control 68 (5) (1997) 971–996.
[16] H. Sira-Ramírez, A general canonical form for feedback passivity of nonlinear systems, Int. J. Control 71 (5) (1998) 891–905.
[17] K. Fujimoto, K. Sakurama, T. Sugie, Trajectory tracking of port-controlled Hamiltonian systems via generalized canonical transformations, Automatica 39 (12) (2003) 2059–2069.

[18] B. Maschke, A. Van der Schaft, B.C. Breedveld, An intrinsic Hamiltonian formulation of network dynamics: Non-standard Poisson structures and gyrators, J. Franklin Inst. 329 (5) (1992) 923–966.
[19] B. Maschke, R. Ortega, A. Van der Schaft, Energy-based Lyapunov functions for forced Hamiltonian systems with dissipation, IEEE Trans. Autom. Control 45 (8) (2000) 1498–1502.
[20] C. Batlle, Passive control theory I and II, in: The 2nd EURON/GEOPLEX Summer School on Modeling and Control of Complex Dynamical Systems, July (2005) 18-22, Bertinoro, Italy, 2005.
[21] N. Monshizadeh, P. Monshizadeh, R. Ortega, A. Van der Schaft, Conditions on shifted passivity of port-Hamiltonian systems, Systems Control Lett. 123 (2019) 55–61.
[22] Y. Wang, C. Li, D. Cheng, Generalized Hamiltonian realization of time-invariant nonlinear systems, Automatica 39 (8) (2003) 1437–1443.
[23] C.A. Farschman, K.P. Viswanath, B.E. Ydstie, Process systems and inventory control, AIChE J. 44 (8) (1998) 1841–1857.
[24] N.H. Hoang, B.E. Ydstie, Integration of inventory control into the port-Hamiltonian framework for dissipative stabilization of chemical reactors, Asian J. Control (2022) http://dx.doi.org/10.1002/asjc.2668.
[25] R. Antonelli, A. Astolfi, Continuous stirred tank reactors: Easy to stabilise? Automatica 39 (10) (2003) 1817–1827.
[26] H. Ramírez, D. Sbarbaro, R. Ortega, On the control of non-linear processes: An IDA-PBC approach, J. Proc. Control 19 (3) (2009) 405–414.
[27] C. Batlle, R. Ortega, D. Sbarbaro, H. Ramírez, Corrigendum to on the control of non-linear processes: An IDA-pbc approach, J. Proc. Control 20 (1) (2010) 121–122.
[28] T.S. Nguyen, N.H. Hoang, M.A. Hussain, Feedback passivation plus tracking-error-based multivariable control for a class of free-radical polymerization reactors, Int. J. Control 92 (9) (2019) 1970–1984.
[29] T.S. Nguyen, C.K. Tan, N.H. Hoang, M.A. Hussain, Tracking-error-based control of a chemical reactor using decoupled dynamic variables, IFAC-PapersOnLine 52 (7) (2019) 74–79.
[30] T.S. Nguyen, N.H. Hoang, M.A. Hussain, Tracking error plus damping injection control of non-minimum phase processes, IFAC-PapersOnLine 51 (18) (2018) 643–648.
[31] T.S. Nguyen, N.H. Hoang, M.A. Hussain, C.K. Tan, Tracking-error control via the relaxing port-Hamiltonian formulation: Application to level control and batch polymerization reactor, J. Proc. Control 80 (2019) 152–166.
[32] A. Yaghmaei, M.J. Yazdanpanah, Trajectory tracking for a class of contractive port Hamiltonian systems, Automatica 83 (2017) 331–336.
[33] R. Stadlmayr, M. Schöberl, K. Schlacher, A combination of feedforward and feedback for the control of the nonlinear benchmark inertia wheel pendulum, in: Proceedings of the European Control Conference, ECC, Greece, 2007, pp. 5802–5808.
[34] M. Schöberl, K. Schlacher, On an intrinsic formulation of time-variant port-Hamiltonian systems, Automatica 48 (2012) 2194–2200.
[35] D. Jeltsema, J.M.A. Scherpen, A dual relation between port-Hamiltonian systems and the brayton-moser equations for nonlinear switched RLC circuits, Automatica 39 (6) (2003) 969–979.
[36] A. Favache, D. Dochain, J.J. Winkin, Power-shaping control: Writing the system dynamics into the Brayton-Moser form, Systems Control Lett. 60 (8) (2011) 618–624.
[37] M. Guay, N. Hudon, Stabilization of nonlinear systems via potential-based realization, IEEE Trans. Autom. Control 61 (4) (2016) 1075–1080.
[38] F. Dörfler, J.K. Johnsen, F. Allgöwer, An introduction to interconnection and damping assignment passivity-based control in process engineering, J. Proc. Control 19 (9) (2009) 1413–1426.
[39] H. Hoang, P. Mai, D. Dochain, On the relaxing dissipation of dissipative pseudo hamiltonian models, IFAC-PapersOnLine 48 (8) (2015) 1051–1056.
[40] H. Ramírez, B. Maschke, D. Sbarbaro, Irreversible port-Hamiltonian systems: A general formulation of irreversible processes with application to the CSTR, Chem. Eng. Sci. 89 (2013) 223–234.
[41] H. Hoang, F. Couenne, Y.Le. Gorrec, C.L. Chen, B.E. Ydstie, Passivity-based nonlinear control of CSTR via asymptotic observers, Annu. Rev. Control 37 (2) (2013) 278–288.
[42] H. Olsson, K.J. Åström, C.C. De Wit, M. Gäfvert, P. Lischinsky, Friction models and friction compensation, Eur. J. Control 4 (3) (1998) 176–195.
[43] H. Olsson, K.J. Åström, Friction generated limit cycles, IEEE Trans. Control Syst. Technol. 9 (4) (2001) 629–636.
[44] V.T. Pham, C. Volos, T. Kapitaniak, Systems without equilibrium, in: Systems with Hidden Attractors: from Theory to Realization in Circuits, in: SpringerBriefs in Applied Sciences and Technology, Springer, Cham, 2017, pp. 51–63, http://dx.doi.org/10.1007/978-3-319-53721-4.
[45] T.F. Edgar, D.M. Himmelblau, L.S. Lasdon, Optimization of Chemical Processes, second ed., McGraw-Hill, New York, 2007.
[46] T.S. Nguyen, C.K. Tan, N.H. Hoang, M.A. Hussain, D. Bonvin, A perturbed port-Hamiltonian approach for the stabilization of homogeneous reaction systems via the control of vessel extents, Comput. Chem. Eng. 154 (2021) 107458.
[47] R. Reyes-Báez, A.Van.der. Schaft, B. Jayawardhana, Tracking control of fully-actuated port-Hamiltonian mechanical systems via sliding manifolds and contraction analysis, IFAC-PapersOnLine 50 (1) (2017) 8256–8261.
[48] R. Reyes-Báez, Virtual Contraction and Passivity Based Control of Nonlinear Mechanical Systems: Trajectory Tracking and Group Coordination, (Ph.D. thesis), University of Groningen, 2019, http://dx.doi.org/10.33612/diss.96171118.
[49] R. Ortega, A. Van der Schaft, B. Maschke, G. Escobar, Interconnection and damping assignment passivity-based control of port-controlled Hamiltonian systems, Automatica 38 (4) (2002) 585–596.